(2)

ARL-TR-91-8

Copy No. 27

NONSTATIONARY HIGHER ORDER SPECTRAL ANALYSIS

Technical Report under Contract N00014-89-J-1967

Gary R. Wilson
Keith R. Hardwicke

APPLIED RESEARCH LABORATORIES
THE UNIVERSITY OF TEXAS AT AUSTIN
POST OFFICE BOX 8029, AUSTIN, TEXAS 78713-8029

23 April 1991

Technical Report

Prepared for:

OFFICE OF THE CHIEF OF NAVAL RESEARCH
DEPARTMENT OF THE NAVY
ARLINGTON, VA 22217-5000

Monitored by:

SPACE AND NAVAL WARFARE SYSTEMS COMMAND
DEPARTMENT OF THE NAVY
WASHINGTON, D.C. 20363-5100

REPORT DOCUMENTATION PAGE

Form Approved
OMB No. 0704-0188

1. AGENCY USE ONLY (Leave blank)	2. REPORT DATE	3. REPORT TYPE AND DATES COVERED
	23 Apr 91	technical

4. TITLE AND SUBTITLE
Nonstationary Higher Order Spectral Analysis

5. FUNDING NUMBERS
N00014-89-J-1967

6. AUTHOR(S)
Wilson, Gary R. Hardwicke, Keith R.

7. PERFORMING ORGANIZATION NAMES(S) AND ADDRESS(ES)
Applied Research Laboratories
The University of Texas at Austin
P.O. Box 8029
Austin, Texas 78713-8029

8. PERFORMING ORGANIZATION REPORT NUMBER
ARL-TR-91-8

9. SPONSORING/MONITORING AGENCY NAME(S) AND ADDRESS(ES)
Office of the Chief of Naval Research
Department of the Navy
Arlington, Virginia 22217-5000

Space and Naval Warfare
Systems Command
Department of the Navy
Washington, D.C. 20363-5100

10. SPONSORING/MONITORING AGENCY REPORT NUMBER

11. SUPPLEMENTARY NOTES

12a. DISTRIBUTION/AVAILABILITY STATEMENT
Approved for public release; distribution is unlimited.

12b. DISTRIBUTION CODE

13. ABSTRACT (Maximum 200 words)
In this report we discuss the detection performance of a variety of higher order spectra for a variety of signals. Of particular significance is the introduction of a new type of higher order spectra called nonstationary higher order spectra. Nonstationary higher order spectra are not the stationary higher order spectral representations of nonstationary processes, but are in fact different spectra which contain the stationary higher order spectra as a subset of their domain. It is shown quantitatively through theoretical predictions and simulations that these type of spectra perform better at detecting nonstationary signals than do the traditional stationary spectra. For the first time, small sample statistics have been derived and applied to the detection performance rather than asymptotic statistics, resulting in a more accurate performance prediction for typical sample sizes for nonstationary signals.

14. SUBJECT TERMS
(see reverse side)

15. NUMBER OF PAGES
70

16. PRICE CODE

17. SECURITY CLASSIFICATION OF REPORT	18. SECURITY CLASSIFICATION OF THIS PAGE	19. SECURITY CLASSIFICATION OF ABSTRACT	20. LIMITATION OF ABSTRACT
UNCLASSIFIED	UNCLASSIFIED	UNCLASSIFIED	SAR

14. higher order spectrum
bispectrum
power spectrum
harmonic
cumulant spectrum
spectral correlation
spectral processing
transient
polyspectrum
cross power spectrum
signal processing
nonstationary

TABLE OF CONTENTS

Page

LIST OF FIGURES v

EXECUTIVE SUMMARY

1. HIGHER ORDER SPECTRAL ANALYSIS 1
   - 1.1 INTRODUCTION 1
   - 1.2 THEORY OF HIGHER ORDER SPECTRAL PROCESSING 1
     - 1.2.1 Cumulant Functions 1
     - 1.2.2 The Functional Approach to Higher Order Spectra 2
     - 1.2.3 The Statistical Approach to Higher Order Spectra 3
   - 1.3 ESTIMATION OF HIGHER ORDER SPECTRA 4
   - 1.4 EXAMPLES OF SPECTRAL DENSITY FUNCTIONS 5
     - 1.4.1 The Auto and Cross Power Spectrum 5
     - 1.4.2 The Nonstationary Power Spectrum: Spectral Correlation 6
     - 1.4.3 The Auto and Cross Bispectrum 6
2. COMPARISON OF THE NARROWBAND DETECTION PERFORMANCE OF THE AUTO AND CROSS POWER SPECTRUM 9
   - 2.1 ESTIMATION OF THE CROSS POWER SPECTRUM 9
   - 2.2 EFFECTS OF NOISE ON THE CROSS POWER SPECTRUM ESTIMATE 11
   - 2.3 COMPARISON TO THE AUTO POWER SPECTRUM 12
3. COMPARISON OF THE DETECTION PERFORMANCE OF THE POWER SPECTRUM AND SPECTRAL CORRELATION 33
   - 3.1 ESTIMATION OF THE SPECTRAL CORRELATION FOR DETECTION OF NARROWBAND HARMONICS 33
   - 3.2 DETECTION OF NARROWBAND HARMONICS 38
   - 3.3 DETECTION OF A WEAK TONE IN THE PRESENCE OF A STRONGER HARMONIC 43
   - 3.4 DETECTION OF TRANSIENTS USING THE SPECTRAL CORRELATION AND POWER SPECTRUM 50
4. COMPARISON OF THE DETECTION PERFORMANCE OF THE POWER SPECTRUM AND BISPECTRUM 55
   - 4.1 ESTIMATION OF THE BISPECTRUM 55
   - 4.2 DETECTION OF HARMONIC COMPONENTS USING THE BISPECTRUM 56

REFERENCES 65

LIST OF FIGURES

Figure		Page
2.1	Auto Power Spectrum Detection Performance	17
2.2	Cross Power Spectrum Detection Performance	19
2.3	Comparison of Auto and Cross Power Spectrum Detection Performance	21
2.4	Asymptotic Detection Performance, L=1000	27
2.5	Auto and Cross Power Spectrum Comparison	29
3.1	Comparison of Exact and Asymptotic False Alarm Rates for Ten Averages	36
3.2	Comparison of Power Spectrum and Spectral Correlation for Narrowband Harmonic Detection, Ten Averages	39
3.3	Comparison of Power Spectrum and Spectral Correlation for Narrowband Harmonic Detection, Four Averages	41
3.4	Comparison of Power Spectrum and Spectral Correlation for Detecting a Weak Harmonic in the Presence of a Stronger Harmonic, Four Averages	45
3.5	Comparison of Power Spectrum and Spectral Correlation for Detecting a Weak Harmonic in the Presence of a Stronger Harmonic, Ten Averages	47
3.6	Gain of Spectral Correlation for Low Signal-to-Noise Ratio Tone	49
3.7	Comparison of Power Spectrum and Spectral Correlation Transient Detection Performance	52
4.1	False Alarm Probability as a Function of Normalized Bispectrum Threshold	58
4.2	Comparison of Bispectrum and Power Spectrum Transient Detection Performance	61

EXECUTIVE SUMMARY

In this report we discuss the detection performance of a variety of higher order spectra for a variety of signals. Of particular significance is the introduction of a new type of higher order spectra called *nonstationary* higher order spectra. Nonstationary higher order spectra are not the stationary higher order spectral representations of nonstationary processes, but are in fact different spectra which contain the stationary higher order spectra as a subset of their domain. It is shown quantitatively through theoretical predictions and simulations that these type of spectra perform better at detecting nonstationary signals than do the traditional stationary spectra. For the first time, small sample statistics have been derived and applied to the detection performance rather than asymptotic statistics, resulting in a more accurate performance prediction for typical sample sizes.

The use of cross power spectrum and auto power spectrum to detect narrowband signals is examined first. Even though the cross and auto power spectra are not higher order spectra, the issue addressed here is whether or not cross-channel processing can increase detection performance commensurate with higher order spectral processing. In an incoherent noise field, the cross power spectrum of the noise asymptotically approaches zero, so it should achieve some processing gain over auto power spectrum processing for narrowband signals. However, it is shown that if the cross power spectrum is applied to the half beams of a towed array and the auto power spectrum is applied to the full beam of a towed array, then in an isotropic noise field the cross power spectrum actually performs about 1 dB worse than the auto power spectrum. This result is due to the fact that the noise levels in the half beams are approximately 3 dB more than the noise level in the full beam due to the decreased directionality of the half beams. Thus cross power spectrum processing does not result in improved detection performance over the auto power spectrum.

Having determined that cross-channel processing does not result in any detection gains for certain sensor systems of interest to the Navy, we then restrict our attention to single channel processing and examine the detection performance of the auto power spectrum compared to various auto higher order spectra. We consider the case of narrowband detection when two harmonically related narrowband components are present. Higher order spectra are designed to detect distinct frequency components that are coherently related. Two narrowband harmonics can be considered as a specific case of a cyclo-stationary process, so we first examine the detection performance of the

nonstationary power spectrum, which is related by a simple transform to the spectral correlation. We derive correctly for the first time the small sample density function for the magnitude of the spectral correlation and use this function to predict the probability of detecting a pair of harmonically related narrowband components as a function of signal to noise ratio at a specified false alarm rate. We show that the spectral correlation will perform significantly better than the power spectrum, but that it is necessary to use the unnormalized spectral correlation rather than the normalized spectral correlation to achieve this improvement. In addition, we examine the detection performance of the bispectrum and show that it also performs better than the power spectrum when the unnormalized bispectrum is used.

We also consider the case of finite duration (transient) signals and compare the detection performance of the spectral correlation (nonstationary power spectrum) and stationary power spectrum. We derive for the first time the small sample density function for the spectral correlation when the transient signal is considered to be a single deterministic (but unknown) waveform. In this case the spectral correlation also performs better than the power spectrum.

In summary, we show that when we wish to detect *nonstationary* signals such as harmonically related narrowband components or finite duration transients, our newly defined *nonstationary* higher order spectra perform better at detecting these nonstationary processes than do stationary spectra. In this report the gains we have demonstrated have been based on very simple processing procedures. More appropriate processing procedures can be developed that will result in even more processing gain than has been demonstrated here.

1. HIGHER ORDER SPECTRAL ANALYSIS

1.1 INTRODUCTION

In this report we discuss the detection performance of a variety of higher order spectra. Of special significance is the introduction of nonstationary higher order spectra and their application to detection of nonstationary signals. In this section we introduce new terminology: *polyspectrum* refers to a stationary higher order spectrum and *cumulant spectrum* refers to a nonstationary higher order spectrum. This terminology, first suggested by Melvin Hinich, is contrary to convention, in which polyspectrum and cumulant spectrum are used interchangeably, but this distinction appears to be a natural one when the concept of nonstationary higher order spectra is introduced.

This first section gives an overview of stationary and nonstationary higher order spectra from both a functional and a statistical perspective. The functional approach will be used to define the stationary higher order spectrum, or polyspectrum, and the statistical approach will be used to define nonstationary higher order spectra, or cumulant spectrum. Estimation of higher order spectra is discussed, and expressions for several stationary and nonstationary spectra are given. The following sections demonstrate quantitatively the detection performance for various higher order spectral estimates.

1.2 THEORY OF HIGHER ORDER SPECTRAL PROCESSING

1.2.1 Cumulant Functions

Higher order spectra of a random process are often referred to as cumulant spectra. The nth order cumulant function of a J-length vector random process whose components are $X_{h(i)}(t_i)$, h(i) = 1. . . J, i = 1 . . . n, is defined in terms of the characteristic function of the random process by

$$[X_{h(1)}(t_1), \ldots, X_{h(n)}(t_n)]_n = (-1)^n \frac{\delta^n \ln \Phi(a_{h(1),1}, \ldots, a_{h(n),n})}{\delta a_{h(1),1} \ldots \delta a_{h(n),n}} \Bigg|_{a_{h(1),1} = \ldots a_{h(n),n} = 0} , \quad (1.1)$$

where the characteristic function is defined as

$$\Phi(a_{h(1),1}, \ldots, a_{h(n),n}) = \left\langle \exp\left\{ i\left(a_{h(1),1} X_{h(1)}(t_1) + \ldots + a_{h(n),n} X_{h(n)}(t_n)\right)\right\}\right\rangle . \quad (1.2)$$

The square brackets [ ] denote the cumulant function. One property of the characteristic function is that if any subset of the $X_{h(i)}(t_i)$ are independent of the rest of the $X_{h(i)}(t_i)$, then the characteristic function factors. For example, if $X_{h(1)}(t_1), \ldots, X_{h(r)}(t_r)$ is independent of $X_{h(r+1)}(t_{r+1}), \ldots, X_{h(n)}(t_n)$, then the characteristic function is

$$\Phi(a_{h(1)}, \ldots, a_{h(n)}) = \Phi(a_{h(1)}, \ldots, a_{h(r)})\Phi(a_{h(r+1)}, \ldots, a_{h(n)}) \quad . \tag{1.3}$$

If the characteristic function factors, then the nth partial derivative of the characteristic function given in Eq. (1.1) is zero and the cumulant function is thus zero. This demonstrates an important property of the cumulant function: the nth order cumulant function is nonzero only when there is statistical dependence between the n elements of the cumulant function.

1.2.2 The Functional Approach to Higher Order Spectra

There are two approaches to the theory of higher order spectra based on cumulants: the functional approach and the statistical approach. We will discuss first the functional approach. If the random process $X_{h(i)}(t)$ is stationary, then there exists a process $Z_{h(i)}(\omega)$ with orthogonal increments such that

$$X_{h(i)}(t) = \int_{-\infty}^{\infty} e^{it\omega} dZ_{h(i)}(\omega) \quad . \tag{1.4}$$

If the random process is nonstationary, then either the process $Z_{h(i)}(\omega)$ does not have orthogonal increments or the kernel function cannot be $e^{it\omega}$. In this report we will confine the functional approach to the case of stationary processes. In this case, the nth order cumulant of the vector random process is a function only of time differences and can be written using the spectral representation given in Eq. (1.4) as

$$\begin{aligned} &\left[X_{h(1)}(t),\, X_{h(2)}(t+\tau_1), \ldots,\, X_{h(n)}(t+\tau_{n-1})\right]_n = \\ &\int_{-\infty}^{\infty} \cdots \int_{-\infty}^{\infty} e^{i(\omega_1+\ldots+\omega_n)t} e^{i(\omega_1\tau_1+\ldots+\omega_{n-1}\tau_{n-1})} \left[dZ_{h(1)}(\omega_1), \ldots, dZ_{h(n)}(\omega_n)\right]_n \quad . \end{aligned} \tag{1.5}$$

The nth order cumulant of the $X_{h(i)}(t)$ is nonzero only when the nth order cumulant of the orthogonal increments $dZ_{h(i)}(\omega)$ is nonzero. However, because the increments are orthogonal, their cumulant is nonzero only if all of the n frequencies are not distinct.

Furthermore, because $X_{h(i)}(t)$ is stationary, its nth order cumulant is independent of t, which is true in general only for the case $\omega_1 + \ldots + \omega_n = 0$ due to the presence of the exponential $e^{i(\omega_1+\ldots+\omega_n)t}$ in the integral. This case satisfies the requirement that the n frequencies not be all distinct. Thus the nth order cumulant of the $X_{h(i)}(t)$ is

$$\begin{aligned}&[X_{h(1)}(t),\, X_{h(2)}(t+\tau_1),\, \ldots,\, X_{h(n)}(t+\tau_{n-1})]_n = \\ &\int_{-\infty}^{\infty} \ldots \int_{-\infty}^{\infty} e^{i(\omega_1\tau_1+\ldots+\omega_{n-1}\tau_{n-1})}[dZ_{h(1)}(\omega_1),\, \ldots,\, dZ_{h(n)}(-\omega_1 - \ldots - \omega_{n-1})]_n\end{aligned} \tag{1.6}$$

for $\omega_1 + \ldots + \omega_n = 0$, and zero otherwise.

If we now define a function $P_{h(1),\ldots,h(n)}(\omega_1, \ldots, \omega_{n-1})$ such that

$$\begin{aligned}&dP_{h(1),\ldots,h(n)}\,(\omega_1, \ldots, \omega_{n-1}) = \\ &[dZ_{h(1)}(\omega_1), \ldots, dZ_{h(n-1)}(\omega_{n-1}), dZ_{h(n)}(-\omega_1 \ldots -\omega_{n-1})]_n\ ,\end{aligned} \tag{1.7}$$

then if $P_{h(1),\ldots,h(n)}$ is continuous it can be written as

$$dP_{h(1),\ldots,h(n)}(\omega_1, \ldots, \omega_{n-1}) = p_{h(1),\ldots,h(n)}(\omega_1, \ldots, \omega_{n-1})d\omega_1 \ldots d\omega_{n-1}\ , \tag{1.8}$$

and Eq. (1.6) can be written as

$$\begin{aligned}&[X_{h(1)}(t),\, X_{h(2)}(t+\tau_1),\, \ldots,\, X_{h(n)}(t+\tau_{n-1})]_n = \\ &\int_{-\infty}^{\infty} \ldots \int_{-\infty}^{\infty} e^{i(\omega_1\tau_1+\ldots+\omega_{n-1}\tau_{n-1})} p_{h(1),\ldots,h(n)}(\omega_1, \ldots, \omega_{n-1})d\omega_1 \ldots d\omega_{n-1} = \\ &\Im_{n-1}^{-1}\{p_{h(1),\ldots,h(n)}(\omega_1, \ldots, \omega_{n-1})\}\ .\end{aligned} \tag{1.9}$$

Thus the nth order cumulant of the $X_{h(i)}(t)$ is the inverse Fourier transform of the function $p_{h(1),\ldots,h(n)}$. This function is referred to as the nth order polyspectral density function of the $X_{h(i)}(t)$. If the cumulant function is integrable, then the nth order spectral density function can be written as the Fourier transform of the cumulant function:

$$p_{h(1),\ldots,h(n)}(\omega_1, \ldots, \omega_{n-1}) = \Im_{n-1}\{[X_{h(1)}(t), \ldots, X_{h(n)}(t+\tau_{n-1})]_n\}\ . \tag{1.10}$$

1.2.3 The Statistical Approach to Higher Order Spectra

The previous section has described a functional approach to stationary higher order spectra, or polyspectra. We will now consider an alternative statistical approach. Given a

vector valued discrete time series whose nth order cumulant exists and is finite, then the nth order discrete Fourier transform of the cumulant exists and we can thus define an nth order cumulant spectral density function as the nth order discrete Fourier transform of the cumulant spectral density function:

$$p_{h(1),\ldots,h(n)}(\omega_1, \ldots, \omega_n) = \sum_{t_1, \ldots, t_n = -\infty}^{\infty} [X_{h(1)}(t_1), \ldots, X_{h(n)}(t_n)]_n e^{-i(\omega_1 t_1 + \ldots + \omega_n t_n)} \quad . \tag{1.11}$$

Notice that no assumption of stationarity has been made. For this nonstationary case we refer to the higher order spectrum defined in Eq. (1.11) as the *cumulant* spectral density function, and we reserve the term *polyspectrum* to refer to the stationary higher order spectrum. This terminology is contrary to convention, in which the terms cumulant spectrum and polyspectrum are used interchangeably. However, when considering nonstationary higher order spectra, it seems useful to make this distinction. For the case of a stationary vector time series, the polyspectrum is defined as (Brillinger, 1975)

$$p_{h(1),\ldots,h(n)}(\omega_1, \ldots, \omega_{n-1}) = \sum_{\tau_1, \ldots, \tau_{n-1} = -\infty}^{\infty} [X_{h(1)}(t), \ldots, X_{h(n)}(t+\tau_{n-1})]_n e^{-i(\omega_1 \tau_1 + \ldots + \omega_{n-1}\tau_{n-1})} \quad . \tag{1.12}$$

1.3 ESTIMATION OF HIGHER ORDER SPECTRA

Brillinger (1975) has shown that if $X_{h(i)}(\omega)$ is the finite Fourier transform of the stationary vector valued discrete time series $X_{h(i)}(t)$,

$$X_{h(i)}(\omega) = \sum_{t=0}^{N-1} X_{h(i)}(t)\, e^{-i\omega t} \quad , \tag{1.13}$$

then the cumulant of the finite Fourier transforms is proportional to the nth order polyspectral density function plus lower order terms:

$$[X_{h(1)}(\omega_1), X_{h(2)}(\omega_2), \ldots, X_{h(n)}(-\omega_1 - \omega_2 \ldots - \omega_{n-1})]_n = N p_{h(1),\ldots,h(n)}(\omega_1, \ldots, \omega_{n-1}) + O(1) \quad . \tag{1.14}$$

However, this result can be extended to nonstationary processes as well. In this case, the cumulant of the finite Fourier transforms is proportional to the nth order cumulant spectral density function plus lower order terms:

$$[X_{h(1)}(\omega_1),\ldots, X_{h(n)}(\omega_n)]_n = Np_{h(1),\ldots,h(n)}(\omega_1,\ldots, \omega_n) + O(1) \quad . \tag{1.15}$$

For stationary processes, the cumulant spectrum is zero except in the domain for which $\omega_1 + \ldots + \omega_n = 0$. Within this domain, the cumulant spectrum is equal to the polyspectrum.

Equations (1.14) and (1.15) form the basis for non-parametric estimation of higher order spectra that will be discussed in more detail in a later section. For the case of the bispectrum, see Hinich (1982). Parametric methods for estimating the bispectrum have also been developed; see, for example, Nikias and Pan (1988). It should be noted that Eqs. (1.14) and (1.15) demonstrate that, as a result of the independence property of the cumulants discussed above, the higher order spectrum is zero unless the Fourier transforms are statistically dependent.

1.4 EXAMPLES OF SPECTRAL DENSITY FUNCTIONS

1.4.1 The Auto and Cross Power Spectrum

The lowest order spectral density function (n=2) is just the power spectrum. For a zero mean stationary process X(t) the second order cumulant is equal to the second order expected value:

$$[X(t),X(t+\tau)]_2 = \langle X(t)X(t+\tau)\rangle = R(\tau) \quad . \tag{1.16}$$

Equation (1.10) then yields the familiar definition of the power spectrum as the Fourier transform of the autocorrelation function $R(\tau)$. Equation (1.14) yields the expression for the power spectrum in terms of the expected value of the magnitude squared of the discrete finite Fourier transform of the time series:

$$\langle X(\omega)X(-\omega)\rangle = \langle |X(\omega)|^2\rangle = Np(\omega) + O(1) \quad . \tag{1.17}$$

For a two-element vector valued zero mean time series the second order cumulant is equal to the crosscorrelation function:

$$[X_1(t),X_2(t+\tau)]_2 = \langle X_1(t)X_2(t+\tau)\rangle = R_{12}(\tau) \quad . \tag{1.18}$$

The cross power spectrum is thus the Fourier transform of the crosscorrelation function and can be estimated from the product of the discrete finite Fourier transforms of the two time series:

$$\langle X_1(\omega)X_2(-\omega)\rangle = \langle X_1(\omega)X_2^*(\omega)\rangle = Np_{12}(\omega) + O(1). \quad (1.19)$$

1.4.2 The Nonstationary Power Spectrum: Spectral Correla on

The n=2 cumulant spectrum, which we will refer to as the nonstationary power spectrum, is related to the expected value of the product of the discrete finite Fourier transform of a zero mean process by Eq. (1.15):

$$\langle X(\omega_1)X(\omega_2)\rangle = Np(\omega_1,\omega_2) + O(1) \quad . \quad (1.20)$$

The nonstationary power spectrum is zero for $\omega_2 \neq -\omega_1$ if the time series is stationary. For $\omega_2 = -\omega_1$ it is equivalent to the power spectrum. The nonstationary power spectrum can be used to detect nonstationary processes by observing non-zero values in the domain for which $\omega_2 \neq -\omega_1$. The nonstationary power spectrum is related to the more familiar spectral correlation $s(\omega_1,\omega_2)$ by the transform

$$p(\omega_1,\omega_2) = s(\omega_1,-\omega_2) \quad . \quad (1.21)$$

1.4.3 The Auto and Cross Bispectrum

The next higher order spectral density function (n=3) is the bispectrum. For a zero mean process the third order cumulant is equal to the third order expected value, so for the bispectrum Eq. (1.10) simplifies to the two-dimensional Fourier transform of the bicovariance function:

$$B(\omega_1,\omega_2) = \Im_2\{\langle X(t)X(t+\tau_1)X(t+\tau_2)\rangle\} \quad . \quad (1.22)$$

The bispectrum is related to the expected value of the triple product of the discrete finite Fourier transform by

$$\langle X(\omega_1)X(\omega_2)X^*(\omega_1+\omega_2)\rangle = NB(\omega_1,\omega_2) + O(1) \quad . \quad (1.23)$$

For a two-element vector valued stationary zero mean time series, the cross-bispectrum is the two-dimensional Fourier transform of the cross-bicovariance:

$$B_{112}(\omega_1,\omega_2) = \Im_2\{\langle X_1(t)X_1(t+\tau_1)X_2(t+\tau_2)\rangle\} \quad . \quad (1.24)$$

The cross-bispectrum is similarly related to the discrete finite Fourier transform of the two time series by

$$\left\langle X_1(\omega_1)X_1(\omega_2)X_2^*(\omega_1+\omega_2)\right\rangle = NB_{112}(\omega_1,\omega_2) + O(1) \quad . \qquad (1.25)$$

2. COMPARISON OF THE NARROWBAND DETECTION PERFORMANCE OF THE AUTO AND CROSS POWER SPECTRUM

Sonar systems usually beamform arrays of hydrophones and process the beamformed signal to perform the initial detection of acoustic sources. Frequently both a full beam (using the full aperture of the array) and two half beams (each using half the full aperture of the array) are formed. One can consider performing the detection operation by either applying auto power spectrum processing to the full beam signal or applying cross power spectrum processing to the half beam signals. The potential advantage of using the cross power spectrum is that if the noise is incoherent between the half beams, then the cross power spectrum of the noise is asymptotically zero. This suggests that the cross power spectrum may be able to detect signals at lower signal-to-noise ratios than the auto power spectrum. In this section we will analytically compare the detection performance of the auto and cross power spectrum to determine if there is any processing gain to be realized by using cross-channel processing.

2.1. ESTIMATION OF THE CROSS POWER SPECTRUM

The cross power spectrum can be estimated from a discrete Fourier transform (DFT) of the data. For the discrete time series x(t), t=0, 1, . . . , N-1, the DFT is given by

$$X(j) = \frac{1}{N} \sum_{t=0}^{N-1} x(t)\, e^{\frac{-i2\pi jt}{N}}, \quad j = 0, 1, \ldots, N-1 \quad . \tag{2.1}$$

The frequency associated with the jth component is

$$\begin{aligned} f_j &= \frac{j}{N} f_s, \; j = 0, 1, \ldots \frac{N}{2} \\ &= \frac{-(N-j)}{N} f_s, \; j = \frac{N}{2} + 1, \cdots, N-1 \quad , \end{aligned} \tag{2.2}$$

where f_s is the rate at which the time series was sampled. The DFT is typically computed using an FFT algorithm. Note that Eq. (2.1) differs from Eq. (1.13) by a factor of 1/N, and thus the following spectral estimates also differ from those in Section 1.

The cross power spectrum is estimated from the DFT by

$$\hat{P}_{12}(f_j) = NX_1(j)X_2^*(j) \quad . \tag{2.3}$$

This estimate is asymptotically unbiased. That is, its expected value approaches the true value of the cross power spectrum as the sample size (the DFT length N) increases (see Eq. (1.19)):

$$\langle \hat{p}_{12}(f_j) \rangle = p_{12}(f_j) + O(N^{-1}) \quad . \tag{2.4}$$

However, the variance of this estimate does not approach zero as the sample size increases but rather approaches a constant value that is the product of the two auto power spectra:

$$\mathrm{VAR}(\hat{p}_{12}) = p_{11}(f_j)p_{22}(f_j) + O(N^{-1}) \quad . \tag{2.5}$$

Thus the estimate given by Eq. (2.3) is not a consistent estimate of the cross power spectrum. For this reason several cross power spectrum estimates are usually averaged in time to produce a consistent estimate:

$$\hat{p}_{12}(f_j) = \frac{1}{L} \sum_{i=1}^{L} N X_1^{(i)}(j) X_2^{(i)*}(j) \quad . \tag{2.6}$$

Frequency averaging can also be used to produce a consistent estimate. If each individual estimate is independent, then the averaged estimate is unbiased with a variance that approaches zero as the number of terms in the average increases:

$$\mathrm{VAR}(\hat{p}_{12}) = \frac{1}{L} p_{11}(f_j)p_{22}(f_j) + O((LN)^{-1}) \quad . \tag{2.7}$$

Independence of each individual estimate for narrowband processing implies that the DFT length is matched to the bandwidth of the narrrowband component being detected.

If we define $\rho_{12}(f_j)$ such that

$$\rho_{12}(f_j) = \frac{p_{12}(f_j)}{\sqrt{p_{11}(f_j)p_{22}(f_j)}} \quad , \tag{2.8}$$

then the estimate of $|\rho_{12}(f_j)|$ given by

$$|\hat{\rho}_{12}(f_j)| = \frac{|\hat{p}_{12}(f_j)|}{\sqrt{\hat{p}_{11}(f_j)\hat{p}_{22}(f_j)}} \quad , \tag{2.9}$$

has a density function given by (Brillinger, 1975)

$$\frac{2L|2L\hat{\rho}_{12}(f_j)|^L}{\Gamma(L)2^{L-1}\left(1-|\rho_{12}(f_j)|^2\right)} I_0\left(|2L\hat{\rho}_{12}(f_j)|\frac{|\rho_{12}(f_j)|}{\left(1-|\rho_{12}(f_j)|^2\right)}\right) K_{L-1}\left(\frac{|2L\hat{\rho}_{12}(f_j)|}{\left(1-|\rho_{12}(f_j)|^2\right)}\right) \quad , \quad (2.10)$$

where I_0 is the modified Bessel function of the first kind of order 0 and K_{L-1} is the modified Bessel function of the second kind of order L-1. Note that this density function is the corrected version of the one that appeared in Brillinger (1975). The function $|\rho_{12}(f_j)|$ is referred to as the coherency spectrum.

2.2 EFFECTS OF NOISE ON THE CROSS POWER SPECTRUM ESTIMATE

The expected value of the cross power spectrum estimate in the presence of noise is given by

$$\left\langle \hat{p}_{12}^{S+N}(f_j) \right\rangle = p_{12}^{S}(f_j) + p_{12}^{N}(f_j) + O\left(N^{-1}\right) , \quad (2.11)$$

that is, the cross power spectrum of the signal plus noise is asymptotically just the sum of the cross power spectra of the signal and the noise. From Eqs. (1.10 and (1.19) it can be seen that if the noise is uncorrelated, its cross power spectrum will be zero. Thus uncorrelated noise asymptotically has no effect on the estimate of the signal's cross power spectrum. If the noise is correlated, it can bias the estimate of the signal's cross power spectrum.

The variance of the cross power spectrum estimate in the presence of noise is given by

$$\begin{aligned} \mathrm{VAR}\left(\hat{p}_{12}^{S+N}(f_j)\right) &= \frac{1}{L}\left(p_{11}^{S}(f_j) + p_{11}^{N}(f_j)\right)\left(p_{22}^{S}(f_j) + p_{22}^{N}(f_j)\right) + O\left((LN)^{-1}\right) \\ &= \frac{1}{L}p_{11}^{S}(f_j)p_{22}^{S}(f_j)\left(1+r_{11}^{-1}(f_j)\right)\left(1+r_{22}^{-1}(f_j)\right) + O\left((LN)^{-1}\right) \quad , \end{aligned} \quad (2.12)$$

where $r_{11}(f_j)$ is the signal-to-noise ratio at the frequency f_j defined as the ratio of the signal power at f_j to the noise power at f_j:

$$r_{11}(f_j) = \frac{p_{11}^{S}(f_j)}{p_{11}^{N}(f_j)} \quad , \quad (2.13)$$

and similarly for $r_{22}(f_j)$. The variance is linearly proportional to the inverse of the averaging time L, i.e., the variance reduces linearly with an increase in the averaging time.

For low signal-to-noise ratios the variance is approximately quadratically proportional to the inverse of the signal-to-noise ratio (assuming that $r_{11}(f_j)$ and $r_{22}(f_j)$ are approximately equal). Thus if the signal-to-noise ratio decreases by 3 dB (1/2), the variance increases by approximately a factor of 4, which can be compensated for by a four-fold increase in the averaging time.

The cross power spectrum can be used to provide an improved estimate of the auto power spectrum of a signal in the presence of noise. If the noise is uncorrelated, then from Eq. (2.11) it can be seen that the expected value of the cross power spectrum of signal plus noise is just equal to the cross power spectrum of the signal. From Eq. (2.8) it can be seen that the cross power spectrum of the signal is related to the auto power spectrum of the signal by the coherency spectrum:

$$\begin{aligned} p^S_{12}(f_j) &= \rho^S_{12}(f_j)\sqrt{p^S_{11}(f_j)p^S_{22}(f_j)} \\ &\cong \rho^S_{12}(f_j)p^S(f_j) \quad , \end{aligned} \tag{2.14}$$

where the approximate equality in the above expression assumes that the signal auto power spectra of the two channels are the same. If the signal of interest is completely coherent (the magnitude of ρ_{12} is 1), then the magnitude of the cross power spectrum of the signal plus noise is asymptotically equal to the auto power spectrum of the signal only. If the signal is only partially coherent, then the magnitude of the cross power spectrum is related to the auto power spectrum by a scale factor that is dependent on the coherency of the signal.

2.3 COMPARISON TO THE AUTO POWER SPECTRUM

If the auto power spectrum is estimated in a manner similar to the cross power spectrum:

$$\hat{p}(f_j) = \frac{1}{L}\sum_{i=1}^{L} NX^{(i)}(j)X^{(i)*}(j) \quad , \tag{2.15}$$

then the expected value of this estimate in the presence of independent noise is

$$\left\langle \hat{p}^{S+N}(f_j) \right\rangle = p^S(f_j) + p^N(f_j) + O\left(N^{-1}\right) \quad , \tag{2.16}$$

and the variance of the estimate is

$$\begin{aligned} \mathrm{VAR}\left(\hat{p}^{S+N}(f_j)\right) &= \frac{1}{L}(p^S(f_j) + p^N(f_j))^2 + O\left((LN)^{-1}\right) \\ &= \frac{1}{L}(p^S(f_j))^2(1+r^{-1}(f_j))^2 + O\left((LN)^{-1}\right) \quad . \end{aligned} \tag{2.17}$$

The density function of the auto power spectrum estimate given by Eq. (2.15) is $p(f_j)\chi^2_{2L}/2L$, where χ^2_{2L} is a chi-square distribution with 2L degrees of freedom. In contrast to the cross power spectrum, the estimate of the signal content of the auto power spectrum is always biased by the presence of noise, even when the noise is uncorrelated.

We now wish to compare the narrowband detection performance of the magnitude of the cross power spectrum computed from the two half beams of a line array and the auto power spectrum computed from the full beam of a line array. Detection is performed with waterfall displays of the auto power spectrum and magnitude of the cross power spectrum. In qualitative terms, a detection occurs when a frequency bin in the waterfall display consistently has an amplitude that is noticeably larger over time than the amplitudes of the neighboring frequency bins. Detection is affected by both the amplitude of the signal in the frequency bin compared to the amplitude of the noise in neighboring frequency bins and the variation of the noise amplitudes in the neighboring frequency bins. If the noise spectrum has large variations over time in the neighborhood of the signal of interest, it can mask the presence of a low level signal. As the variation of the noise amplitudes decreases, it is possible to detect the signal at lower signal amplitudes. Thus detection of narrowband signals with waterfall displays is determined by both the expected value of the signal and noise amplitudes and the variance of the noise.

A detection is said to have occurred when an estimate exceeds a threshold that is determined by the desired false alarm rate. For the auto power spectrum estimate given by Eq. (2.15), the noise only case results in a density function given by $p^N(f_j)\chi^2_{2L}/2L$, where $p^N(f_j)$ is the auto power spectrum of the noise from the full beam of the line array. If a threshold $T(\alpha)$ is determined from the chi-square distribution for a specified false alarm rate α and degrees of freedom 2L, then a detection is said to have occurred when the auto power spectrum estimate exceeds the threshold given by $p^N(f_j)T(\alpha)/2L$.

The probability of detection is the probability that the auto power spectrum estimate will exceed this threshold when a signal is present in addition to the noise, and is dependent on the signal-to-noise ratio. When a signal and noise are present, the auto power spectrum estimate has a density function given by $(r(f_j)+1)p^N(f_j)\chi^2_{2L}/2L$, where $r(f_j)$ is the ratio of the signal power to the noise power from the full beam of the line array. The estimate

$\hat{p}^{S+N}(f_j)$ exceeds the threshold $p^N(f_j)T(\alpha)/2L$ when $2L\hat{p}^{S+N}(f_j)/(r(f_j)+1)p^N(f_j)$ exceeds the value $T(\alpha)/(r(f_j)+1)$. Since $2L\hat{p}^{S+N}(f_j)/(r(f_j)+1)p^N(f_j)$ is distributed χ^2_{2L}, the probability of detection is the probability that a chi-square 2L random variable exceeds the value $T(\alpha)/(r(f_j)+1)$.

If the auto power spectrum is estimated as the magnitude of the cross power spectrum, then the density function for the magnitude of the cross power spectrum is given from Eq. (2.10) as

$$\frac{2}{\sqrt{p_{11}(f_j)p_{22}(f_j)}}\frac{L\left(\frac{L|2\hat{p}_{12}(f_j)|}{\sqrt{p_{11}(f_j)p_{22}(f_j)}}\right)^L}{\Gamma(L)2^{L-1}\left(1-|\rho_{12}(f_j)|^2\right)}I_0\left(\frac{L|2\hat{p}_{12}(f_j)|}{\sqrt{p_{11}(f_j)p_{22}(f_j)}}\frac{|\rho_{12}(f_j)|}{\left(1-|\rho_{12}(f_j)|^2\right)}\right)$$
$$\times K_{L-1}\left(\frac{L|2\hat{p}_{12}(f_j)|}{\sqrt{p_{11}(f_j)p_{22}(f_j)}\left(1-|\rho_{12}(f_j)|^2\right)}\right) \quad , \tag{2.18}$$

where Eq. (2.9) was used to relate the coherence to the cross power spectrum. It is assumed that a consistent estimate of the auto power spectrum of the two half beams is used so that asymptotically the estimates can be replaced by the population values. For the case that (1) the noise is uncorrelated between the two half beams ($\rho^N{}_{12}(f_j) = 0$), (2) the auto power spectrum of the noise is the same on the two half beams, and (3) the half beam noise auto power spectrum is approximately twice the full beam noise auto power spectrum ($p^N{}_{11}(f_j) = p^N{}_{22}(f_j) = 2p^N(f_j)$) due to the different directivity of the full and half beams (assuming isotropic noise), the density function of the magnitude of the cross power spectrum of the noise given by Eq. (2.18) reduces to

$$\frac{1}{p^N(f_j)}\frac{L\left(\frac{L|\hat{p}^N_{12}(f_j)|}{p^N(f_j)}\right)^L}{\Gamma(L)2^{L-1}}K_{L-1}\left(\frac{L|\hat{p}^N_{12}(f_j)|}{p^N(f_j)}\right) \quad . \tag{2.19}$$

From this density function a threshold can be determined for the magnitude of the cross power spectrum that will achieve the desired false alarm rate.

When both signal and noise are present, the coherency spectrum of the signal plus noise is determined by the coherence of the signal, the coherence of the noise, and the signal-to-noise ratio. If the signal is perfectly correlated between the half beams, the noise is uncorrelated, the signal auto power spectrum in the half beams is the same as the signal

auto power spectrum in the full beam (assuming a directional source), and the noise auto power spectrum in the half beams is approximately twice the noise auto power spectrum in the full beam, then applying Eqs. (2.8) and (2.14) results in the magnitude of the coherency spectrum of the signal plus noise equal to $r(f_j)/(r(f_j)+2)$. Under these assumptions, from Eq. (2.18) the density function of the magnitude of the cross power spectrum of signal plus noise is

$$\frac{2}{(r(f_j)+2)p^N(f_j)} \frac{L\left(\frac{L|2\hat{p}_{12}^{S+N}(f_j)|}{(r(f_j)+2)p^N(f_j)}\right)^L}{\Gamma(L)2^{L-1}\left[1-\left(\frac{r(f_j)}{r(f_j)+2}\right)^2\right]} I_0\left(\frac{L|2\hat{p}_{12}^{S+N}(f_j)|}{(r(f_j)+2)p^N(f_j)} \frac{\frac{r(f_j)}{r(f_j)+2}}{\left[1-\left(\frac{r(f_j)}{r(f_j)+2}\right)^2\right]}\right) \times K_{L-1}\left(\frac{L|2\hat{p}_{12}^{S+N}(f_j)|}{(r(f_j)+2)p^N(f_j)\left[1-\left(\frac{r(f_j)}{r(f_j)+2}\right)^2\right]}\right) . \quad (2.20)$$

From this density function the probability of detection can be computed as a function of signal-to-noise ratio.

Shown in Fig. 2.1 is the probability of detection as a function of signal-to-noise ratio for the detector based on the auto power spectrum estimator given by Eq. (2.15). The probability of detection is given for four different averaging lengths L. For the detector based on the magnitude of the cross power spectrum, the probability of detection as a function of signal-to-noise ratio is shown in Fig. 2.2. A comparison of the probability of detection of the auto and cross power spectra is shown in Fig. 2.3. As can be seen, the cross power spectrum requires about a 1 dB higher signal-to-noise ratio than the auto power spectrum to achieve the same probability of detection over a range of signal-to-noise ratios and averaging lengths.

Some insight into the detection performance of the cross power spectrum can be gained by examining the asymptotic distribution of the cross power spectrum. As the number of averages increases, the cross power spectrum estimate given by Eq. (2.6) has a density function that approaches a complex normal density with mean and variance given by Eqs. (2.4) and (2.7) (Brillinger, 1975). Thus the magnitude of the cross power spectrum has an asymptotic Rician density function given by (Papoulis, 1965)

$$\frac{2L|\hat{p}_{12}(f_j)|}{p_{11}(f_j)p_{22}(f_j)} \exp\left[\frac{-L\{|\hat{p}_{12}(f_j)|^2+|p_{12}(f_j)|^2\}}{p_{11}(f_j)p_{22}(f_j)}\right] I_0\left(\frac{2L|\hat{p}_{12}(f_j)||p_{12}(f_j)|}{p_{11}(f_j)p_{22}(f_j)}\right) . \quad (2.21)$$

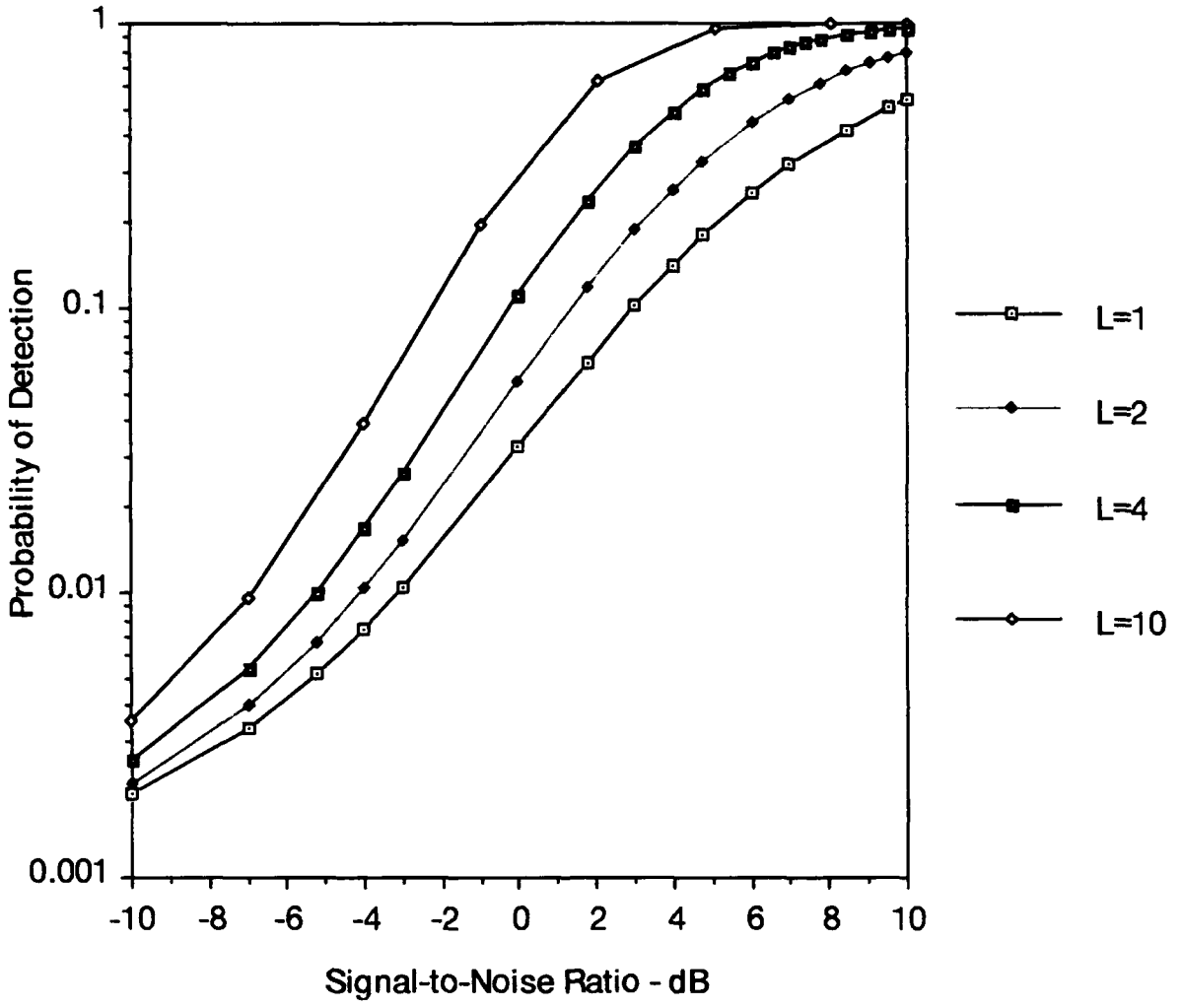

FIGURE 2.1
AUTO POWER SPECTRUM DETECTION PERFORMANCE

AS-91-258

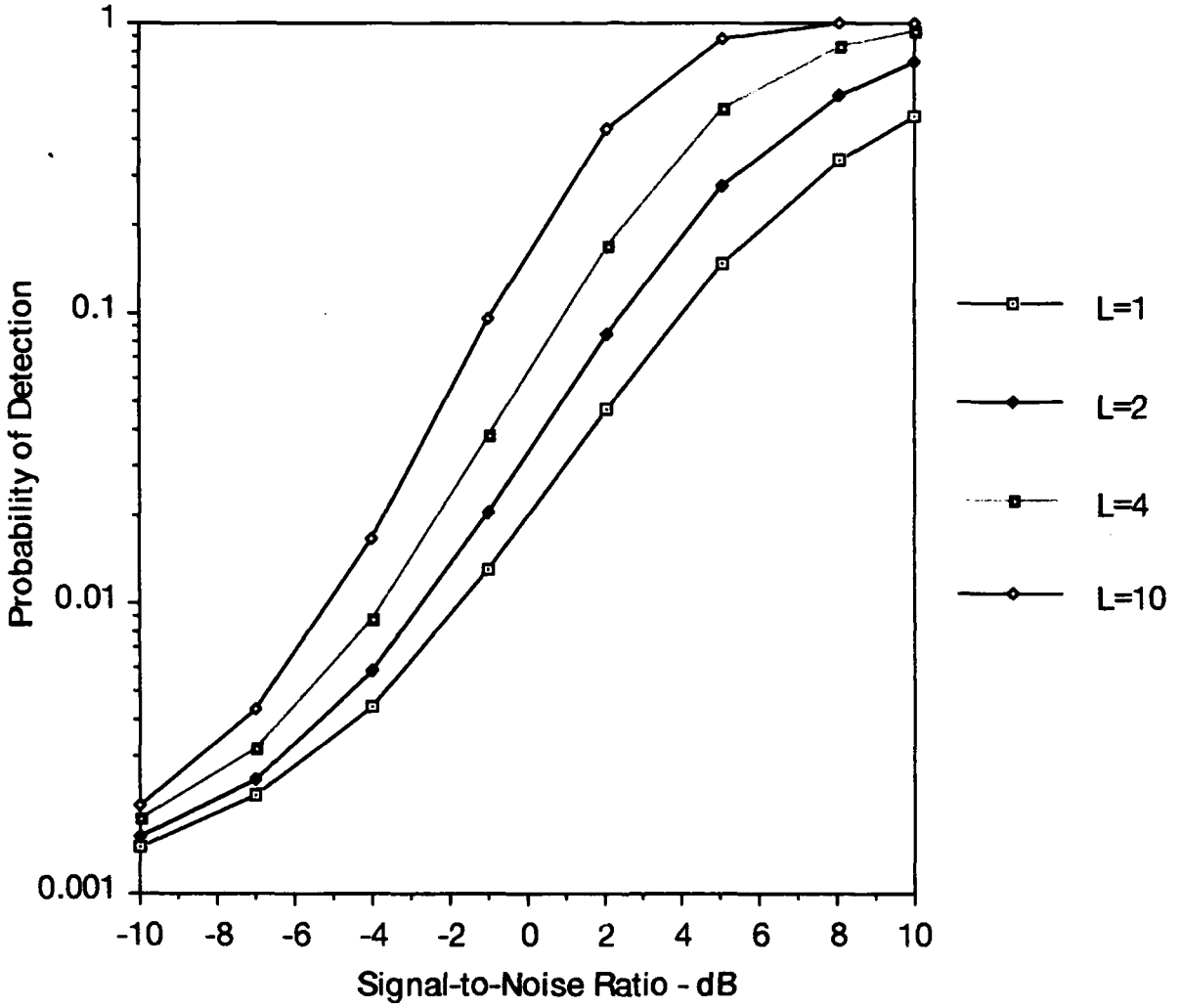

FIGURE 2.2
CROSS POWER SPECTRUM DETECTION PERFORMANCE

AS-91-259

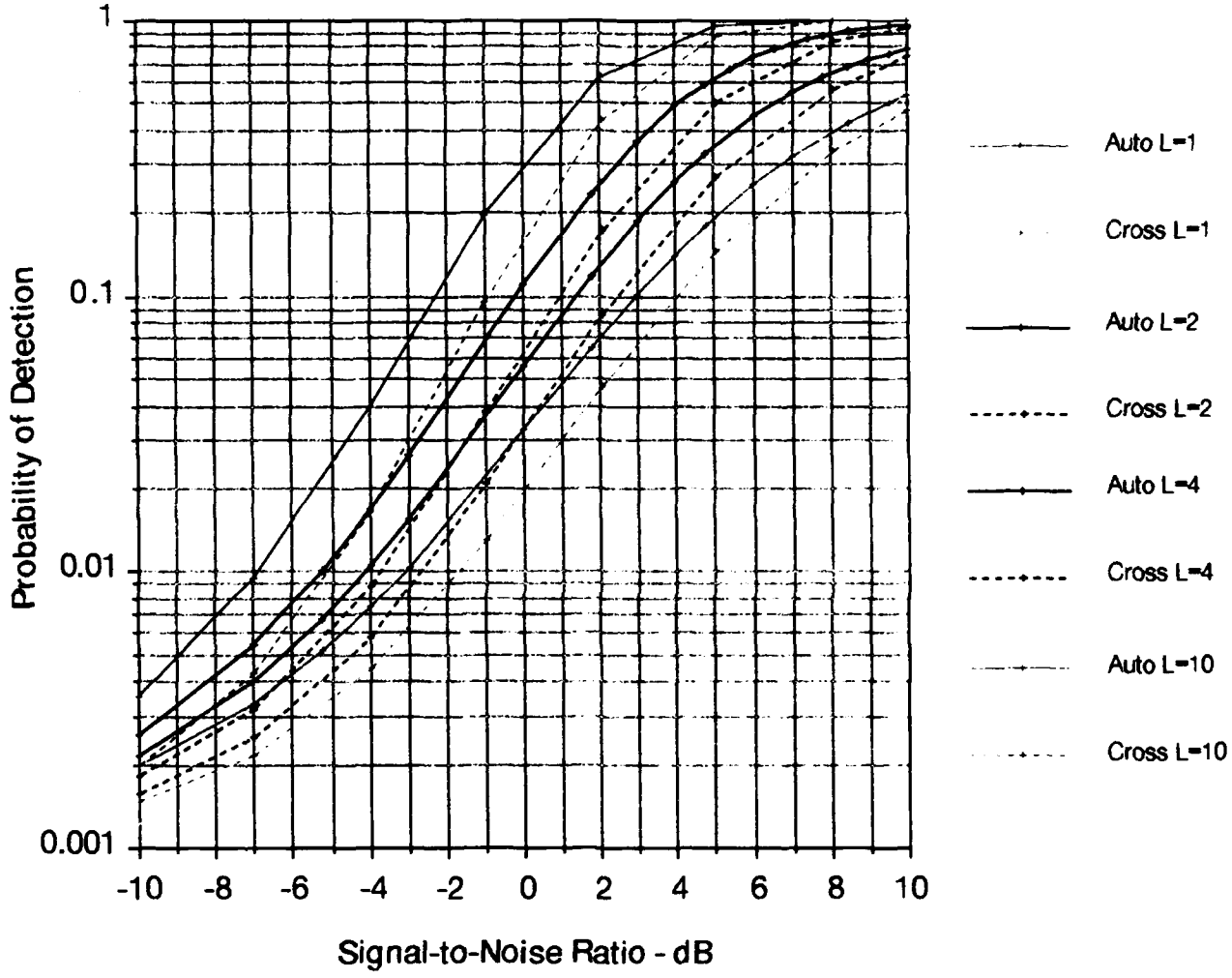

FIGURE 2.3
COMPARISON OF AUTO AND CROSS POWER SPECTRUM
DETECTION PERFORMANCE

AS-90-1002

For the case of noise only, where the noise is uncorrelated and the noise power in the two half beams is approximately equal and twice the noise power in the full beam, then this density reduces to a Rayleigh density given by

$$\frac{L|\hat{p}_{12}(f_j)|}{2(p^N(f_j))^2} \exp\left[\frac{-L|\hat{p}_{12}(f_j)|^2}{4(p^N(f_j))^2}\right] . \tag{2.22}$$

For the signal plus noise case, Eq. (2.21) becomes

$$\frac{2L|\hat{p}_{12}(f_j)|}{(p^N(f_j))^2(r(f_j)+2)^2} \exp\left[\frac{-L\{|\hat{p}_{12}(f_j)|^2 + (p^N(f_j))^2 r^2\}}{(p^N(f_j))^2(r(f_j)+2)^2}\right] I_0\left(\frac{2L|\hat{p}_{12}(f_j)|\, p^N(f_j) r(f_j)}{(p^N(f_j))^2(r(f_j)+2)^2}\right). \tag{2.23}$$

Under the condition that

$$L >> \left(\frac{r+2}{r}\right)^2 , \tag{2.24}$$

that is, when the number of averages L is large ("large" being determined by the signal-to-noise ratio), then Eq. (2.23) has approximately a Gaussian form (Levanon, 1988):

$$\frac{\sqrt{2L}}{\sqrt{2\pi}\, p^N(f_j)\,(r(f_j)+2)} \exp\left[\frac{-2L(\hat{p}(f_j) - p^N(f_j) r(f_j))^2}{2(p^N(f_j)\,(r(f_j)+2))^2}\right] . \tag{2.25}$$

Using these asymptotic densities, the asymptotic mean and variance of the cross power spectrum estimate under both noise and signal plus noise conditions can be compared to the same quantities for the auto power spectrum. This comparison is given in Table 2.1. From a qualitative standpoint, there are two factors that can be seen to reduce the detection performance of the cross power spectrum compared to the auto power spectrum. First, the expected value of the cross power spectrum when noise only is present decreases to zero rather slowly as the number of averages increases, going as $L^{-1/2}$. The separation in the means of the cross power spectrum densities in signal plus noise and noise only cases is at most equal to the signal power spectrum. However, the separation in the means of the auto power spectrum densities is also equal to the signal power spectrum, but independent of the averaging length. Qualitatively, the more an estimate's noise and signal plus noise densities are separated in mean, the better the detection performance. In the case of the cross power spectrum, its means are never separated more than the means of the auto power spectrum. Thus the fact that the cross power spectrum asymptotically goes

to zero for the noise only case does not improve its asymptotic detection performance compared to the auto power spectrum.

TABLE 2.1

COMPARISON OF AUTO AND CROSS POWER SPECTRUM ASYMPTOTIC MEAN AND VARIANCE

	Auto Power Spectrum		Asymptotic Cross Power Spectrum	
	Mean	Variance	Mean	Variance
Noise Only	$p^N(f_j)$	$\frac{(p^N(f_j))^2}{L}$	$p^N(f_j)\sqrt{\frac{\pi}{L}}$	$(4-\pi)\frac{(p^N(f_j))^2}{L}$
Signal-Plus-Noise	$(r(f_j)+1)p^N(f_j)$	$\frac{(p^N(f_j))^2}{L}(r(f_j)+1)^2$	$p^N(f_j)r(f_j)$	$\frac{(p^N(f_j))^2}{L}\frac{(r(f_j)+2)^2}{2}$

Secondly, the asymptotic variance of the cross power spectrum under the noise only case is only slightly smaller than the variance of the auto power spectrum for noise only, which implies that qualitatively the thresholds necessary to achieve a specified false alarm rate are going to be approximately the same. However, the variance of the cross power spectrum for the signal plus noise case is approximately twice as large as the variance of the auto power spectrum of the signal plus noise for low signal-to-noise ratios. Usually, the smaller the variance of an estimate's signal plus noise density, the better the detection performance. This larger variance for the signal plus noise density of the cross power spectrum is due to the fact that the noise power in the half beams is assumed to be twice as large as the noise power in the full beams. It is only at large signal-to-noise ratios, when this factor is insignificant, that the cross power spectrum has a smaller variance than the auto power spectrum. If the noise power in the half beams were the same as the noise power in the full beam, then the cross power spectrum would have a variance that is one half the variance of the auto power spectrum, which would result in better detection for the cross power spectrum. As it is, the larger variance of the cross power spectrum estimate at low signal-to-noise ratios results in reduced detection performance compared to the auto power spectrum estimate.

Shown in Fig. 2.4 is a comparison of the asymptotic detection performance of the auto and cross power spectrum for 1000 averages (L=1000). Even in this asymptotic limit, the auto power spectrum is still performing better than the cross power spectrum.

As a further example of the detection performance of the auto and cross power spectrum, a single narrowband tone was added to uncorrelated noise and fed to the auto and cross power spectrum estimators. For the cross power spectrum the noise is at the same level and independent on the two channels and the same tone is fed into both channels. The power spectrum and the magnitude of the cross power spectrum are shown for different numbers of averages in Fig. 2.5. It should be pointed out that the noise processed by the power spectrum is at the *same* level as the noise processed by the cross power spectrum, not 3 dB lower as would normally be the case when the signals are derived from full and half beam outputs. Thus a more accurate comparison would be to compare the power spectrum performance for a given number of averages to the cross power spectrum performance for one-fourth as many averages.

It can be seen that as the number of averages is increased, the expected value and variance of the magnitude of the cross power spectrum decreases, resulting in noise values that are consistently closer to zero. This results in better detectability of the narrowband component. On the other hand, the noise variance (but not the expected value) of the auto power spectrum is also decreasing as the number of averages increases, resulting in noise values that are consistently closer to their non-zero value. The reduction in the variance of the auto power spectrum estimate also results in better detectability of the narrowband component, even though the noise is non-zero.

The conclusion of this analysis is that even though the cross power spectrum improves the estimate of the amplitude of a narrowband signal, it does not necessarily improve the detectability of that signal due to the increased noise level in the half beam channels compared to the full beam channel. The effects of this increased noise level on detectability can be overcome by increasing the averaging length, but increasing the averaging length also improves the detectability of the auto power spectrum. The cross power spectrum provides a less biased estimate of the narrowband signal than the auto power spectrum, but the auto power spectrum provides a slightly better detection of the narrowband signal.

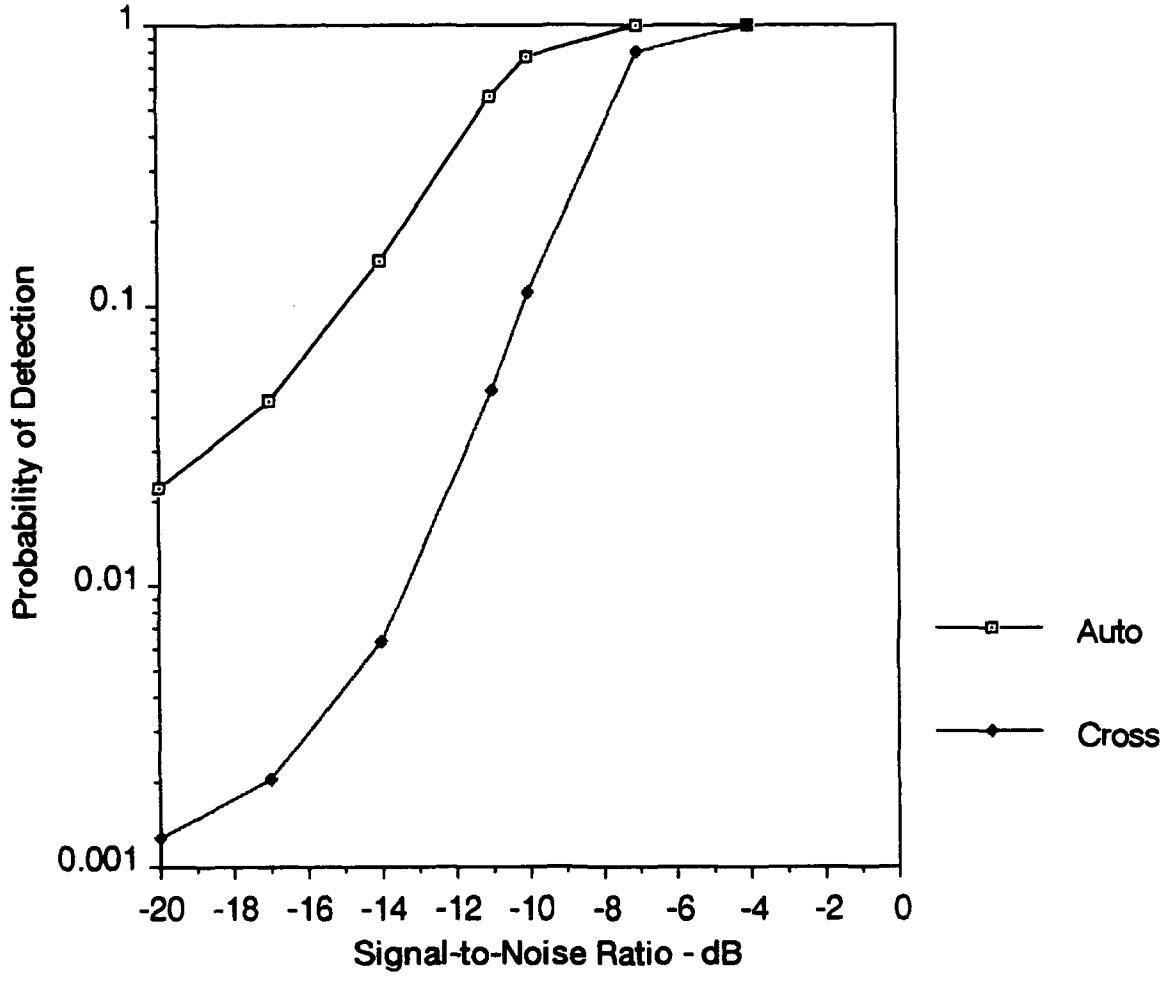

FIGURE 2.4
ASYMPTOTIC DETECTION PERFORMANCE, L=1000

AS-90-1003

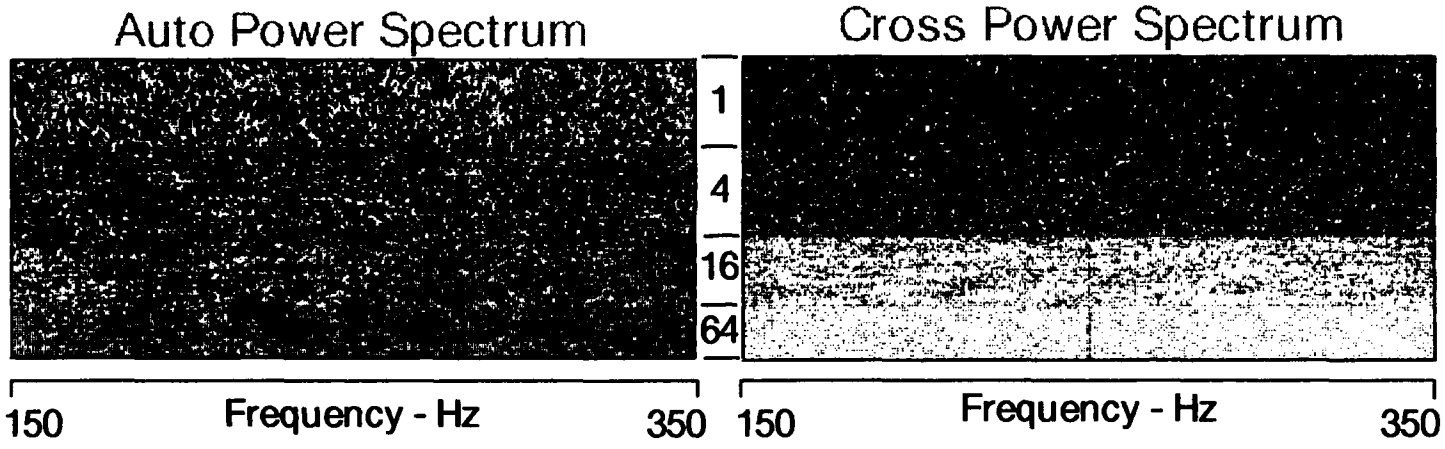

FIGURE 2.5
AUTO AND CROSS POWER SPECTRUM COMPARISON

It should also be pointed out that this analysis did not take into account the effects of visual recognition differential on the detectability of the narrowband component. A more detailed study could indicate the effects of the cross power spectrum on visual recognition differential.

3. COMPARISON OF THE DETECTION PERFORMANCE OF THE POWER SPECTRUM AND SPECTRAL CORRELATION

In Section 2 we demonstrated that there was no processing gain to be realized by cross-channel processing for half-beam sensor systems that have reduced directionality in an isotropic noise field. In Sections 3 and 4 we will consider processing only a single channel such as the output from a full beam beamformer, but we will examine the detection gains that may be realized using higher order spectral processing. In this section we will focus on the spectral correlation, and in Section 4, on the bispectrum. This analysis will concentrate on nonstationary processes. One type of process will be a cyclo-stationary process composed of the sum of narrowband harmonics, and the other will be a finite energy process representing transients. We will compare the detection performance of the power spectrum and the spectral correlation (nonstationary power spectrum) for these two types of processes to determine if using a nonstationary spectrum provides any improvements in detection of nonstationary processes. Similarly to the case of the cross power spectrum, for stationary noise the spectral correlation is zero for distinct frequency components, suggesting the possibility of detection at lower signal-to-noise ratios than would be possible with the power spectrum.

3.1 ESTIMATION OF THE SPECTRAL CORRELATION FOR DETECTION OF NARROWBAND HARMONICS

We will consider two estimates of the spectral correlation, a normalized and an unnormalized estimate. A normalized spectral correlation estimator based on the discrete finite Fourier transform (Eq. (2.1)) is given by

$$\hat{S}(f_i,f_j) = \frac{1}{L}\sum_{k=1}^{L} \frac{NX^{(k)}(f_i)X^{(k)*}(f_j)}{\sqrt{p(f_i)p(f_j)}} \quad . \tag{3.1}$$

Normalization is performed by dividing by the square root of the product of the power spectra at the two frequencies. This estimate is asymptotically unbiased and has a variance that approaches zero as the number of averages increases:

$$VAR\left(\hat{S}(f_i, f_j)\right) = \frac{1}{L} + O\left((LN)^{-1}\right) \quad . \tag{3.2}$$

The estimate given by Eq. (3.1) has a complex Wishart distribution with dimension 2 and degrees of freedom L. The magnitude of the normalized spectral correlation estimator given by Eq. (3.1) has a density function given by (Brillinger, 1975)

$$\frac{2L\left|2L\hat{S}(f_i,f_j)\right|^L}{\Gamma(L)2^{L-1}\left(1-\left|S(f_i,f_j)\right|^2\right)} I_0\left(\left|2L\hat{S}(f_i,f_j)\right|\frac{\left|S(f_i,f_j)\right|}{\left(1-\left|S(f_i,f_j)\right|^2\right)}\right) K_{L-1}\left(\frac{\left|2L\hat{S}(f_i,f_j)\right|}{\left(1-\left|S(f_i,f_j)\right|^2\right)}\right) \quad , \quad (3.3)$$

where I_0 is the modified Bessel function of the first kind of order 0 and K_{L-1} is the modified Bessel function of the second kind of order L-1. Notice that this is the same density function as the one for the coherency spectrum given by Eq. (2.10) and is the corrected version of the one that appeared in Brillinger (1975). For the noise only case where the noise has zero spectral correlation for $f_i \neq f_j$ (stationary noise), this density reduces to

$$\frac{2L\left|2L\hat{S}(f_i,f_j)\right|^L}{\Gamma(L)2^{L-1}} K_{L-1}\left(\left|2L\hat{S}(f_i,f_j)\right|\right) \quad . \quad (3.4)$$

The threshold required to achieve the desired false alarm rate can be calculated from this density. The expected value of the magnitude of the normalized spectral correlation estimate given by Eq. (3.1) for the zero correlation, noise only density given by Eq. (3.4) is

$$\left\langle\left|\hat{S}(f_i,f_j)\right|\right\rangle = \frac{\sqrt{\pi}}{L}\frac{\Gamma(L+\frac{1}{2})}{\Gamma(L)} \quad , \quad (3.5)$$

and the variance is given by

$$\mathrm{VAR}\left\{\left|\hat{S}(f_i,f_j)\right|\right\} = \frac{4}{L} - \left(\frac{\sqrt{\pi}}{L}\frac{\Gamma(L+\frac{1}{2})}{\Gamma(L)}\right)^2 \quad . \quad (3.6)$$

For the case where we are trying to detect two coherently related narrowband tones, if the tones are perfectly coherent spectrally (the normalized spectral correlation is one) and the noise is spectrally incoherent (the normalized spectral correlation is zero), the spectral correlation of the signal plus noise is given by

$$S(f_i, f_j) = \sqrt{\frac{r(f_i)r(f_j)}{(r(f_i)+1)(r(f_j)+1)}} \quad , \quad (3.7)$$

where $r(f_i)$ is the signal-to-noise power ratio:

$$r(f_i) = \frac{p^S(f_i)}{p^N(f_i)} \quad . \quad (3.8)$$

Thus the density function for the signal-plus-noise case is given by

$$\frac{2L\left|2L\hat{S}^{S+N}(f_i,f_j)\right|^L}{\Gamma(L)2^{L-1}\left(1-\frac{r(f_i)r(f_j)}{(r(f_i)+1)(r(f_j)+1)}\right)} I_0\left(\left|2L\hat{S}^{S+N}(f_i,f_j)\right|\frac{\sqrt{(r(f_i)+1)(r(f_j)+1)r(f_i)r(f_j)}}{r(f_i)+r(f_j)+1}\right) \times K_{L-1}\left(\frac{\left|2L\hat{S}^{S+N}(f_i,f_j)\right|}{1-\frac{r(f_i)r(f_j)}{(r(f_i)+1)(r(f_j)+1)}}\right) . \tag{3.9}$$

The spectral correlation estimate given by Eq. (3.1) is asymptotically complex Gaussian, so that for large averages its magnitude has a Rician density given by

$$2L\left|\hat{S}(f_i,f_j)\right| \exp\left[-L\left\{\left|\hat{S}(f_i,f_j)\right|^2+\left|S(f_i,f_j)\right|^2\right\}\right] I_0\left(2L\left|\hat{S}(f_i,f_j)\right|\left|S(f_i,f_j)\right|\right) . \tag{3.10}$$

For the noise only case where the noise is stationary, the spectral correlation of the noise is zero for distinct frequencies. In this case the spectral correlation has a Rayleigh density given by

$$2L\left|\hat{S}(f_i,f_j)\right| \exp\left[-L\left|\hat{S}(f_i,f_j)\right|^2\right] . \tag{3.11}$$

In Fig. 3.1 the false alarm rate that would be computed using the Rayleigh density in Eq. (3.11) is compared to the exact false alarm rate given by the density in Eq. (3.3) for an averaging length of 10(L = 10). The false alarm rate computed from the asymptotic density is underestimated compared to the false alarm rate computed from the exact density. Thus a threshold derived from the asymptotic density would result in a higher false alarm rate than expected. However, for even this short averaging length, the asymptotic false alarm rate for false alarm rates on the order of 10^{-3} is not too different from the exact false alarm rate.

The unnormalized spectral correlation estimate is similar to Eq. (3.1):

$$\hat{s}(f_i,f_j)=\frac{1}{L}\sum_{k=1}^{L} NX^{(k)}(f_i)X^{(k)*}(f_j) , \tag{3.12}$$

where a lower case s is used to denote the unnormalized spectral correlation, and an upper case S is used to denote the normalized version. The density function of the magnitude of the unnormalized spectral correlation is given by

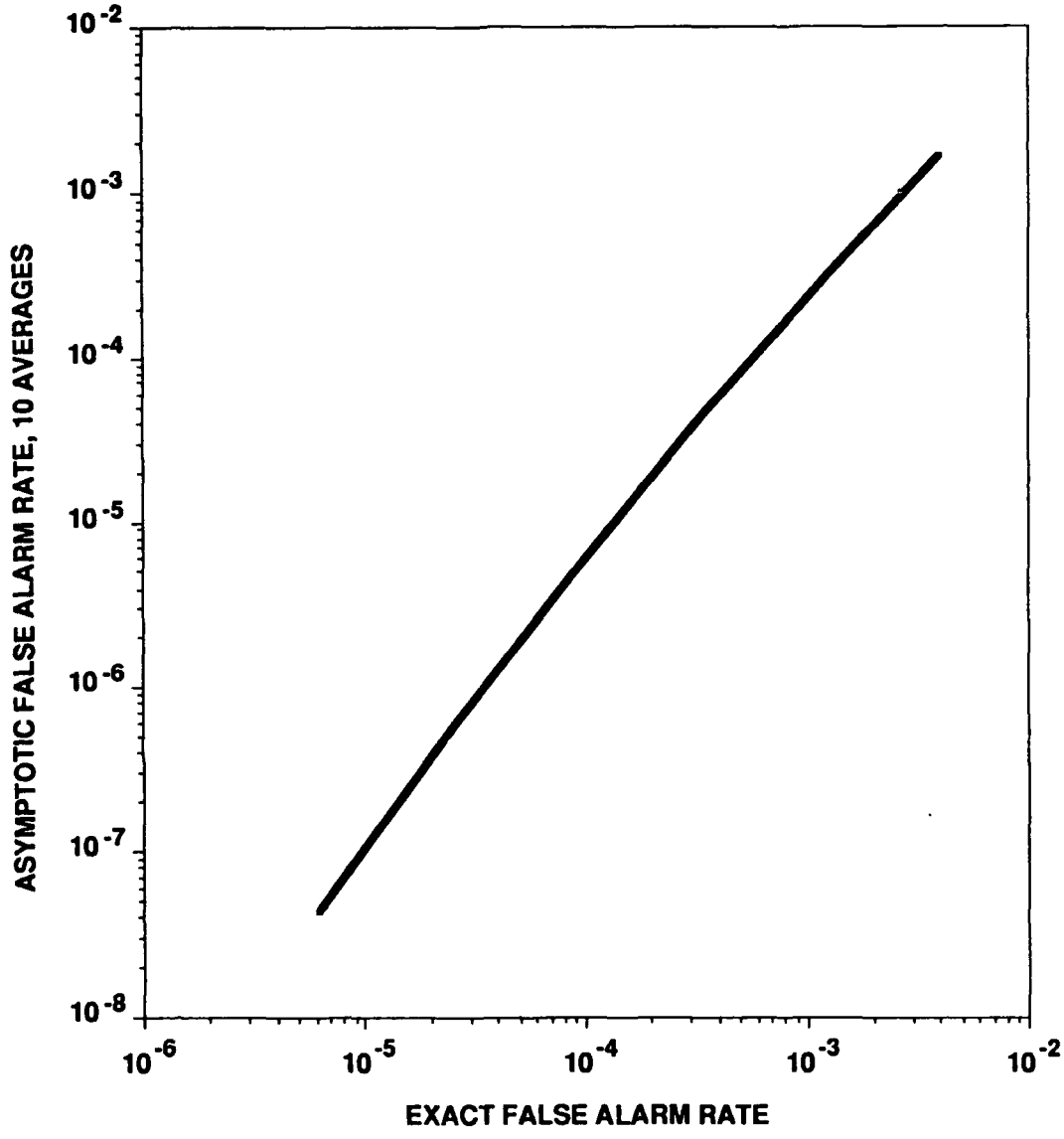

FIGURE 3.1
COMPARISON OF EXACT AND ASYMPTOTIC FALSE ALARM RATES FOR TEN AVERAGES

ARL - UT
AS-91-260
GRW/RFO
5-13-91 50

$$\frac{2L\left|\frac{2L\hat{s}(f_i,f_j)}{\sqrt{p(f_i)p(f_j)}}\right|^L}{\sqrt{p(f_i)p(f_j)}\,\Gamma(L)2^{L-1}\left(1-|S(f_i,f_j)|^2\right)}\, I_0\left(\left|\frac{2L\hat{s}(f_i,f_j)}{\sqrt{p(f_i)p(f_j)}}\right|\frac{|S(f_i,f_j)|}{\left(1-|S(f_i,f_j)|^2\right)}\right)$$
$$\times K_{L-1}\left(\frac{|2L\hat{s}(f_i,f_j)|}{\sqrt{p(f_i)p(f_j)}\left(1-|S(f_i,f_j)|^2\right)}\right) . \tag{3.13}$$

For the noise only case, where the noise is assumed to have no spectral correlation, the density function is

$$\frac{2L\left|\frac{2L\hat{s}(f_i,f_j)}{\sqrt{p^N(f_i)p^N(f_j)}}\right|^L}{\sqrt{p^N(f_i)p^N(f_j)}\,\Gamma(L)2^{L-1}}\, K_{L-1}\left(\left|\frac{2L\hat{s}(f_i,f_j)}{\sqrt{p^N(f_i)p^N(f_j)}}\right|\right) . \tag{3.14}$$

The threshold can be computed for $p^N = 1$, and the threshold for any other value of p^N can be obtained by scaling the $p^N = 1$ threshold by the new value of p^N.

For the signal plus noise case the density function for a coherent signal in stationary noise can be expressed in terms of the signal-to-noise ratio defined in Eq. (3.8) as

$$\frac{2L\left|\frac{2L\hat{s}^{S+N}(f_i,f_j)}{\sqrt{(r(f_i)+1)(r(f_j)+1)p^N(f_i)p^N(f_j)}}\right|^L}{\sqrt{(r(f_i)+1)(r(f_j)+1)p^N(f_i)p^N(f_j)}\,\Gamma(L)2^{L-1}\left(1-\frac{r(f_i)r(f_j)}{(r(f_i)+1)(r(f_j)+1)}\right)}$$
$$\times I_0\left(\left|2L\frac{\hat{s}^{S+N}(f_i,f_j)}{\sqrt{(r(f_i)+1)(r(f_j)+1)p^N(f_i)p^N(f_j)}}\right|\frac{\sqrt{(r(f_i)+1)(r(f_j)+1)\,r(f_i)r(f_j)}}{r(f_i)+r(f_j)+1}\right) \tag{3.15}$$
$$\times K_{L-1}\left(\left|\frac{2L\hat{s}^{S+N}(f_i,f_j)}{\sqrt{(r(f_i)+1)(r(f_j)+1)p^N(f_i)p^N(f_j)}}\right|\Big/\left(1-\frac{r(f_i)r(f_j)}{(r(f_i)+1)(r(f_j)+1)}\right)\right) .$$

To calculate the probabilities associated with the densities given by Eqs. (3.14) and (3.15), the noise power spectrum can arbitrarily be set to 1. In this case the noise only densities for the normalized and unnormalized spectral correlation, Eqs. (3.4) and (3.14), are equivalent. However, the signal plus noise densities given by Eqs. (3.9) and (3.15) are

different. This difference will result in different detection performance for the normalized and unnormalized spectral correlation, as will be seen in the following.

3.2 DETECTION OF NARROWBAND HARMONICS

We will now compare analytically and experimentally the detection performance of the normalized and unnormalized spectral correlation and the power spectrum for the detection of narrowband harmonics in stationary noise. We will first consider the case of two harmonics of equal amplitude and then the case of different amplitudes. A constant false alarm rate of 10^{-3} was used.

Shown in Fig. 3.2 is the probability of detection as a function of signal-to-noise ratio for the power spectrum and both the normalized and unnormalized spectral correlation for the case of two harmonics of equal amplitudes and 10 averages (L = 10). A false alarm rate of 10^{-3} resulted in a threshold value for the normalized spectral correlation of 0.92. The spectral correlation results were calculated using the signal plus noise density function given in Eqs. (3.9) and (3.15), i.e., the Rician approximation for large averages was not used. As can be seen, the normalized spectral correlation performs significantly worse than either the unnormalized spectral correlation or the power spectrum. It is also of interest that the unnormalized spectral correlation provides approximately a 2 dB improvement in detection performance compared to the power spectrum.

Also shown in Fig. 3.2 are the measured probabilities of detection for two coherent tones (100 Hz and 200 Hz) in white Gaussian noise, along with their 90% confidence intervals for the number of observations used. The theoretical thresholds were used, and the 10^{-3} false alarm rate with these thresholds fell well within the 90% confidence interval ($\pm 1 \cdot 10^{-3}$) of the measured false alarm rates. The measured probabilities of detection agree well with the theoretical detection probabilities, with the exception that the normalized spectral correlation is somewhat over-predicted, and confirm the observations that the normalized spectral correlation performs worse than the power spectrum while the unnormalized spectral correlation improves upon the power spectrum detection performance.

Shown in Fig. 3.3 are the same type of results, but with an averaging length of 4 instead of 10. The relative performance of the three types of detectors is the same as for the

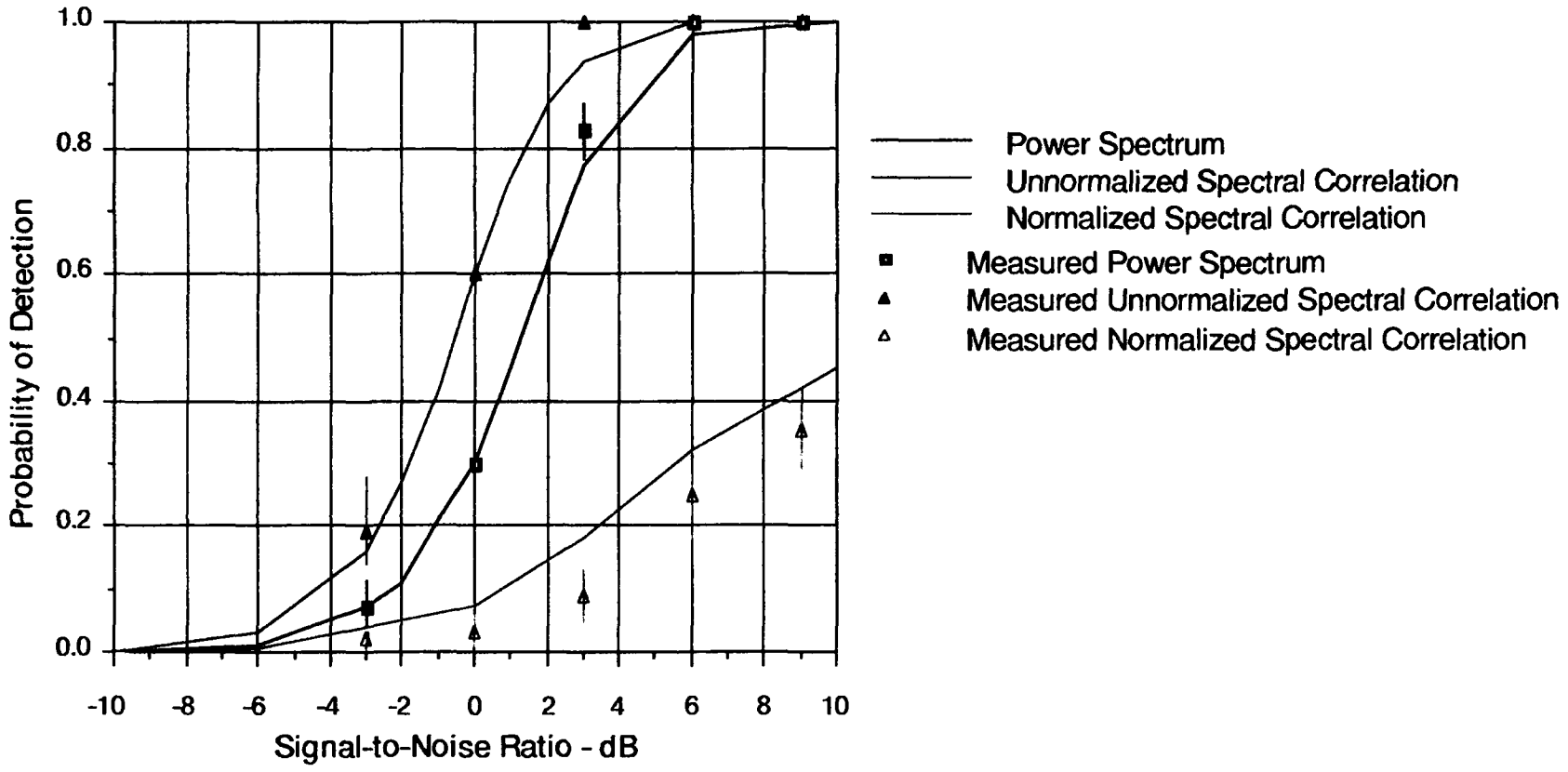

FIGURE 3.2
COMPARISON OF POWER SPECTRUM AND SPECTRAL CORRELATION
FOR NARROWBAND HARMONIC DETECTION, TEN AVERAGES

AS-91-127

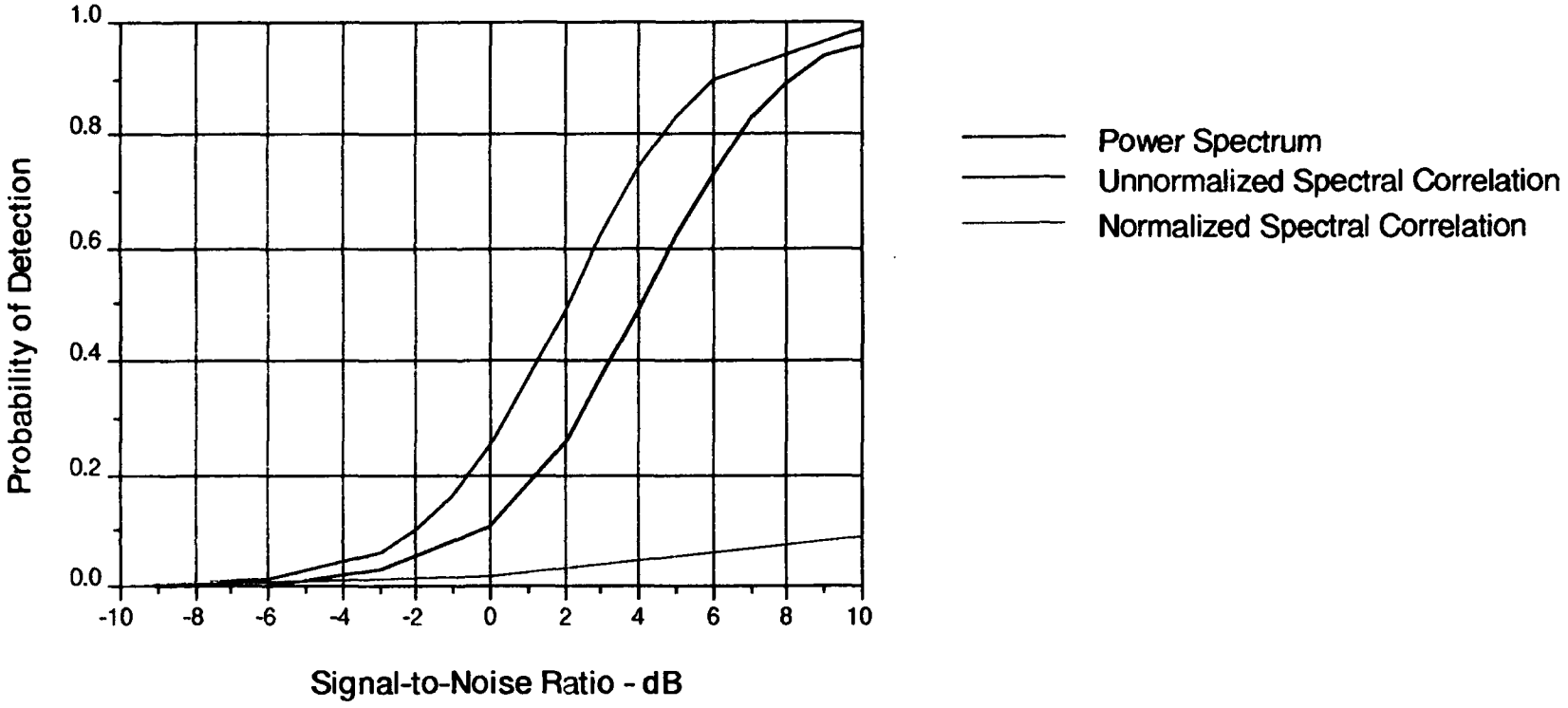

FIGURE 3.3
COMPARSION OF POWER SPECTRUM AND SPECTRAL CORRELATION
FOR NARROWBAND HARMONIC DETECTION, FOUR AVERAGES

3.3 DETECTION OF A WEAK TONE IN THE PRESENCE OF A STRONGER HARMONIC

Now consider the case where a strong tone is present and we wish to detect a weaker tone which is harmonically related to the strong tone. We will start with the unnormalized spectral correlation estimate given in Eq. (3.12). The density function is the same as in Eq. (3.13), but now we need to consider the stronger tone as part of the noise we wish to discriminate against. That is, we are not interested in the detection of the stronger tone, but in the detection of the weaker harmonically related tone in the presence of the stronger tone. In this case the density function for noise only is a modified version of the noise only density function given by Eq. (3.14):

$$\frac{2\left|\frac{2L\hat{s}(f_i,f_j)}{\sqrt{(r(f_i)+1)p^N(f_i)p^N(f_j)}}\right|^L}{\sqrt{(r(f_i)+1)p^N(f_i)p^N(f_j)}\Gamma(L)2^{L-1}} K_{L-1}\left(\left|\frac{2L\hat{s}(f_i,f_j)}{\sqrt{(r(f_i)+1)p^N(f_i)p^N(f_j)}}\right|\right) . \qquad (3.16)$$

In Eq. (3.16) it has been assumed that the stronger tone is at the frequency f_i, so the "noise" at the frequency f_i is the sum of the background noise power denoted $p^N(f_i)$ and the signal power of the stronger tone. The signal power of the stronger tone is included in the signal-to-noise ratio term $r(f_i)$. The result of this modified noise density function is a larger threshold than would be obtained by the noise density function given by Eq. (3.14). The signal plus noise density function is the same as the one given by Eq. (3.15), so it is to be expected that the detection performance would be worse than the detection performance obtained previously for the unnormalized spectral correlation.

Shown in Figs. 3.4 and 3.5 are the performance of the unnormalized spectral correlation for detecting a weak tone in the presence of a stronger harmonic compared to the performance of the power spectrum for detecting the weak tone. Figure 3.4 contains the results for an averaging length of 4, and Fig. 3.5 corresponds to an averaging length of 10. In both these figures the signal-to-noise ratio for the stronger harmonic is 10 dB. For four averages the spectral correlation performs slightly better than the power spectrum only at signal-to-noise ratios below about 3 dB. However, for ten averages the spectral correlation performs better than the power spectrum at signal-to-noise ratios below about 5 dB. Furthermore, there is increased gain at low signal-to-noise ratios compared to the case of four averages. In both averaging cases there is more gain from spectral correlation at lower signal-to-noise ratios than at higher signal-to-noise ratios. Figure 3.6 shows the gain of the

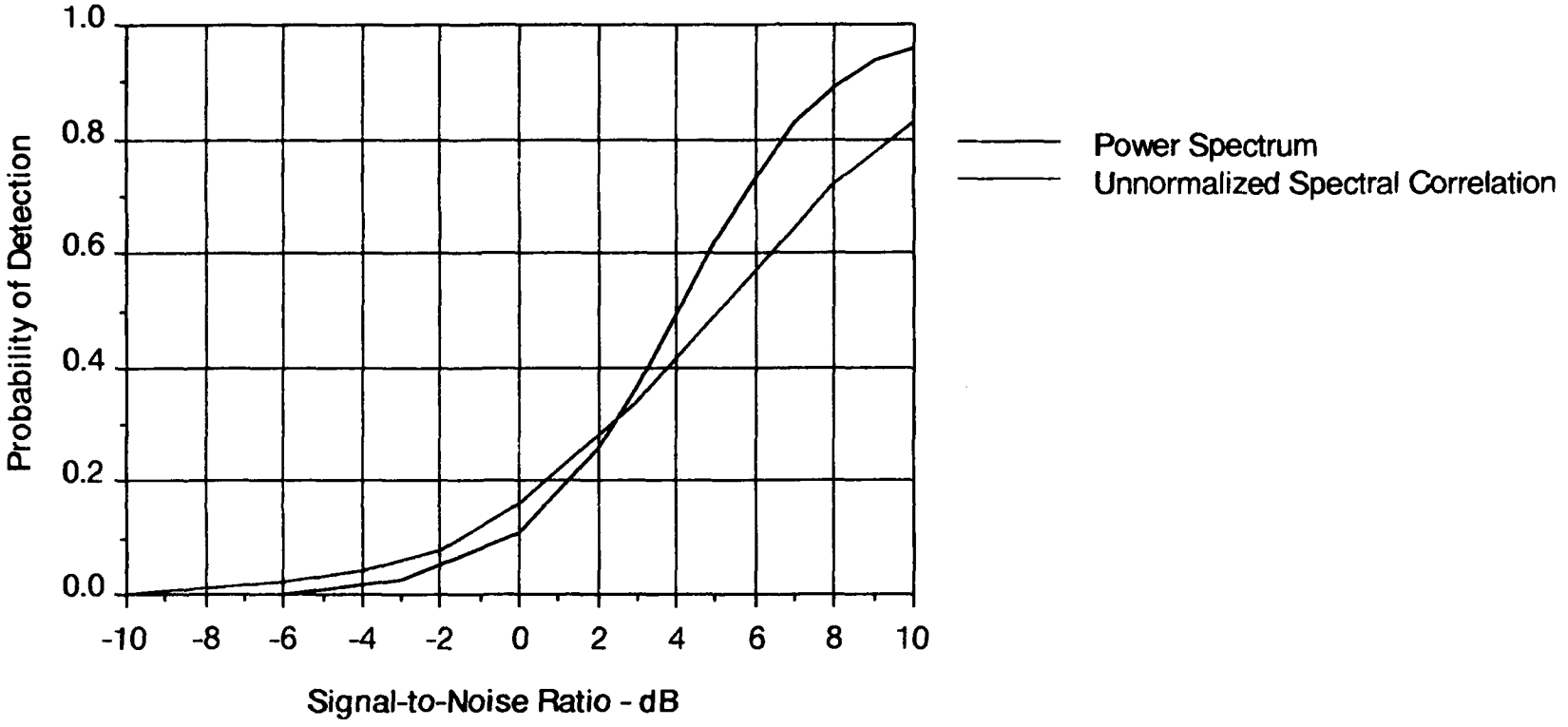

FIGURE 3.4
COMPARISON OF POWER SPECTRUM AND SPECTRAL CORRELATION
FOR DETECTING A WEAK HARMONIC IN THE PRESENCE OF A
STRONGER HARMONIC, FOUR AVERAGES

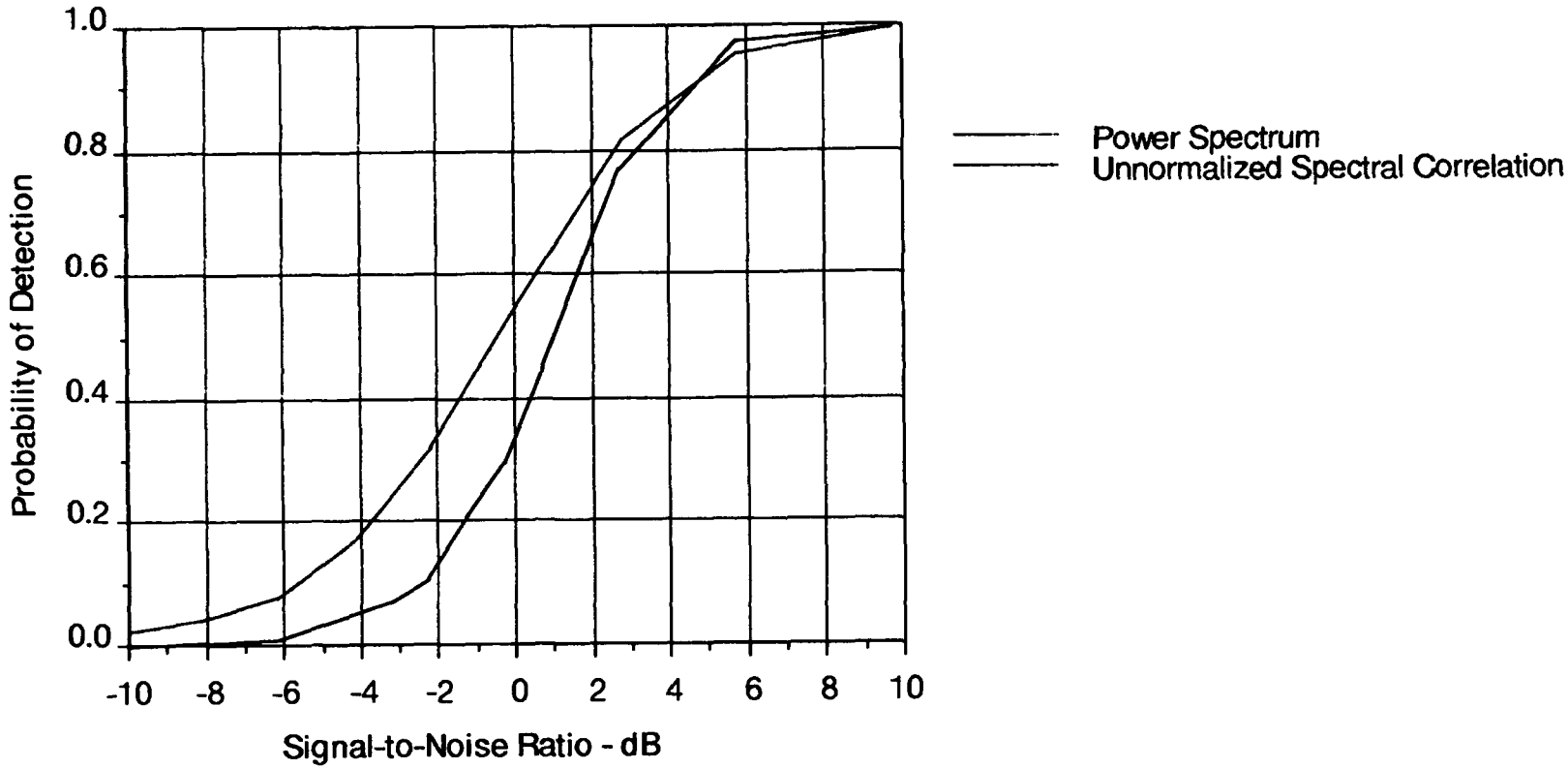

FIGURE 3.5
COMPARISON OF POWER SPECTRUM AND SPECTRAL CORRELATION
FOR DETECTING A WEAK HARMONIC IN THE PRESENCE OF A
STRONGER HARMONIC, TEN AVERAGES

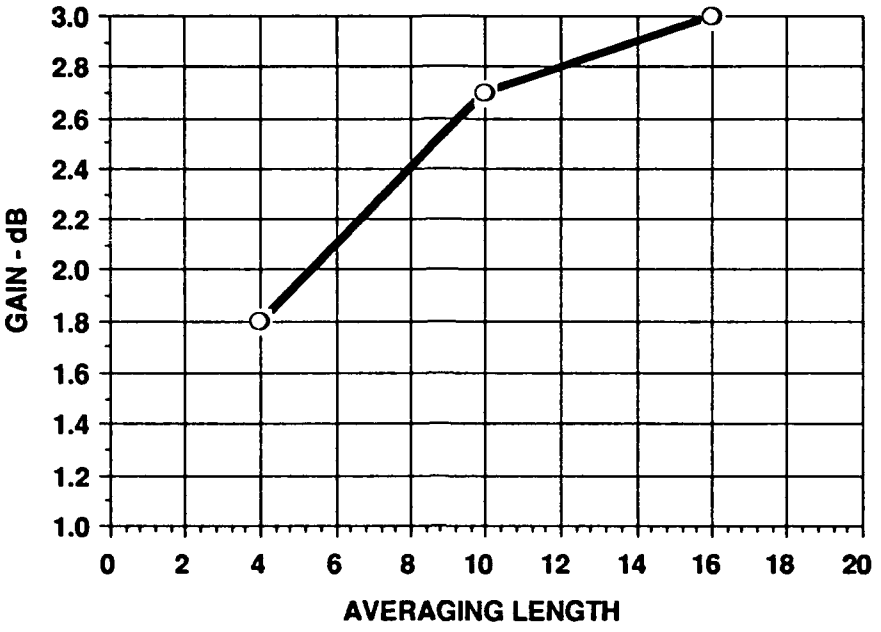

FIGURE 3.6
GAIN OF SPECTRAL CORRELATION
FOR LOW SIGNAL-TO-NOISE RATIO TONE
GAIN IS DEFINED AS THE INCREASE IN SIGNAL-TO-NOISE RATIO REQUIRED FOR THE POWER SPECTRUM TO HAVE THE SAME PROBABILITY OF DETECTION AS THE SPECTRAL CORRELATION.

spectral correlation compared to the power spectrum for three different averaging lengths for a signal-to-noise ratio of -4 dB for the weak tone and 10 dB for the stronger harmonic. The gain is the amount the signal-to-noise ratio must be increased in order for the power spectrum to have the same probability of detection as the spectral correlation. As can be seen, the gain increases as the averaging length increases.

3.4 DETECTION OF TRANSIENTS USING THE SPECTRAL CORRELATION AND POWER SPECTRUM

We will now turn our attention to finite duration signals, or transients, and compare the detection performance of spectral correlation and power spectrum against transients in white Gaussian noise. We will treat our transient signal as a single deterministic event rather than as an ensemble of random events since that is how transient processing is usually performed (i.e., no ensemble averaging). We will then determine the density functions of the spectral correlation and power spectrum for this signal plus noise case.

We will first consider the density function of the power spectrum estimate. The power spectrum is estimated as in Eq. (2.15), but with no time averaging (L=1). For a deterministic signal that has a Fourier transform, the expected value of the power spectrum estimate given by Eq. (2.15) is

$$\langle \hat{p}(f_j) \rangle = p^N(f_j) + N^{-1} e^S(f_j) + O(N^{-1}) \quad , \tag{3.17}$$

where $e^s(f_j)$ is the energy spectrum of the signal given by

$$e^S(f_j) = N^2 |X^s(f_j)|^2 \quad , \tag{3.18}$$

and $X^S(f_j)$ is the N point DFT of the deterministic signal given by Eq. (2.1). For transient detection it is more appropriate to consider the detection statistic as the power spectrum estimate normalized by the known (or estimated) noise power spectrum:

$$\frac{2\hat{p}(f_j)}{p^N(f_j)} \quad . \tag{3.19}$$

The normalized power spectrum estimate given by Eq. (3.19) is distributed $\chi^2_2(\lambda)$, where $\chi^2_2(\lambda)$ is a *non-central* chi-square distribution with 2 degrees of freedom and non-centrality parameter λ. The value of λ is given by

$$\lambda(f_i) = 2\frac{N^{-1}e^{S}(f_j)}{p^{N}(f_j)} = 2\,r(f_i) \quad , \tag{3.20}$$

where

$$r(f_i) = \frac{N^{-1}e^{S}(f_j)}{p^{N}(f_j)} \tag{3.21}$$

is the signal-to-noise ratio. Thus if a transient is considered a deterministic signal, the probability of false alarm for the normalized power spectrum can be computed from a central chi-square distribution and the probability of detection as a function of signal-to-noise ratio can be computed from a non-central chi-square distribution.

Just as we normalized the power spectrum estimate by the noise power, we will also normalize the spectral correlation estimate by the noise power. In this case the normalized spectral correlation estimate for transient detection is

$$\hat{S}(f_i, f_j) = \frac{NX(f_i)X^{*}(f_j)}{\sqrt{p^{N}(f_i)p^{N}(f_j)}} \quad . \tag{3.22}$$

For a deterministic transient, this estimate has a *non-central* complex Wishart distribution of dimension 2 with one degree of freedom. The magnitude of this estimate has a density given by (Baugh and Hardwicke, 1991)

$$4\left|\hat{S}(f_i, f_j)\right| \int_0^{\infty} \frac{1}{y} e^{-\left(\lambda(f_i)+\lambda(f_j) + \left(\left|\hat{S}(f_i,f_j)\right|/y\right)^2 + y^2\right)} I_0\left(\frac{2\left|\hat{S}(f_i,\, f_j)\right|\sqrt{\lambda(f_i)}}{y}\right) I_0\left(2\,y\sqrt{\lambda(f_j)}\right) dy \quad , \tag{3.23}$$

where in this case the noncentrality parameter $\lambda(f_i) = r(f_i)$. Under the noise only case the estimate has a central complex Wishart distribution of dimension 2 and its magnitude has a density given by Eq. (3.3) with L=1.

Shown in Fig. 3.7 is a comparison of the probability of detection of spectral correlation and power spectrum as a function of signal-to-noise ratio for a false alarm rate of 10^{-4}. In this case the signal is considered to be a transient whose energy is equally divided between two frequency bins and is zero elsewhere. The spectral correlation result represents the result from the spectral correlation computed for these two frequency bins. The power spectrum result represents the result of detecting the transient in *either* of the

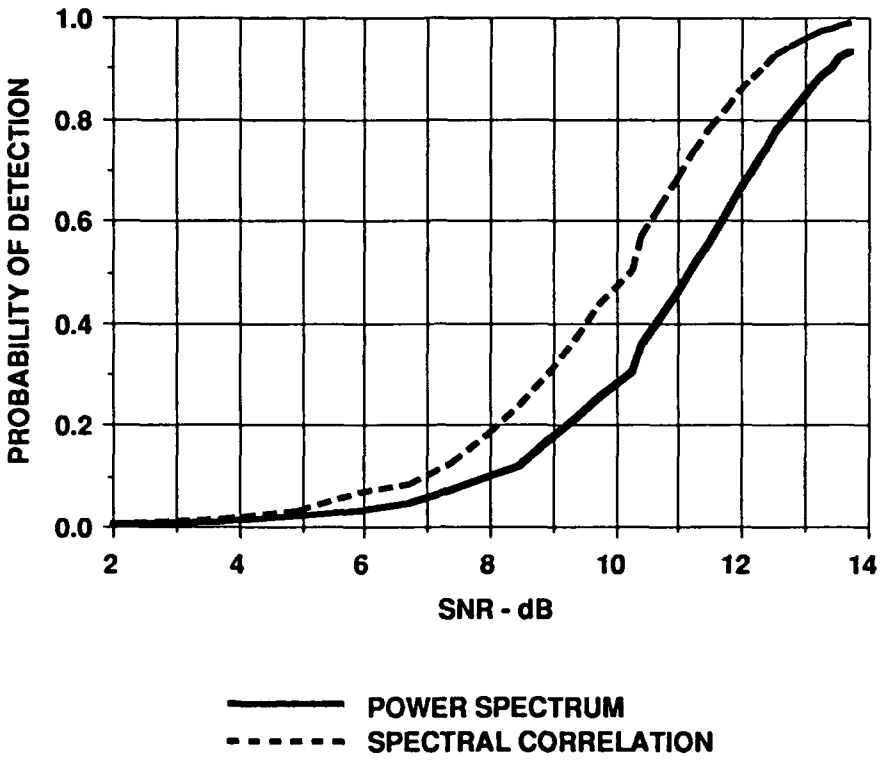

FIGURE 3.7
COMPARISON OF POWER SPECTRUM AND
SPECTRAL CORRELATION TRANSIENT DETECTION PERFORMANCE

two bins. As can be seen, the spectral correlation has a little over a 1 dB detection performance gain compared to the auto power spectrum. This simplistic example is meant to demonstrate only that the use of a nonstationary spectrum can result in more processing gain against a transient than the use of a stationary spectrum. Additional methods for processing the spectral correlation can result in even more gains (Baugh and Hardwicke, 1991).

4. COMPARISON OF THE DETECTION PERFORMANCE OF THE POWER SPECTRUM AND BISPECTRUM

In this section we will examine the performance of the bispectrum for detecting narrowband harmonic components and compare its performance to the power spectrum. We will not examine the nonstationary bispectrum, but will restrict the harmonic components so that they lie within the region of the stationary bispectrum, which is a subset of the region of the nonstationary bispectrum. The results of this analysis can be applied in general to the nonstationary bispectrum. First we will describe the bispectrum estimate and then specify its density function. As with the spectral correlation, we will consider both a normalized and unnormalized bispectrum estimate.

4.1 ESTIMATION OF THE BISPECTRUM

A consistent estimate of the unnormalized bispectrum can be constructed using a DFT (Eq. (2.1)) of the time series. The expected value of the complex function

$$F(j,k) = N^2 X(j) X(k) X^*(j+k) \tag{4.1}$$

is equal to the bispectrum $B(f_j,f_k)$ plus terms on the order of N^{-1}. Thus F(j,k) is an unbiased estimate of the bispectrum. However, it is not a consistent estimate of the bispectrum because its variance increases with N. To obtain a consistent estimate, either the function F(j,k) can be coherently averaged in frequency, or multiple realizations of F(j,k) can be coherently averaged in time, or both. For the case of detection of narrowband harmonics, averaging in time is preferred over averaging in frequency.

The time averaged bispectrum estimate is given by

$$\hat{B}(j,k) = \frac{1}{L} \sum_{i=1}^{L} F_i(j,k) \quad , \tag{4.2}$$

where L is the number of DFTs over which the bispectrum is coherently averaged. If the function given by Eq. (4.1) is uncorrelated in time, then the variance of this estimator is given by

$$\text{VAR } \hat{B}(j,k) = \frac{N}{L} P(f_j) P(f_k) P(f_{j+k}) + O\left(\frac{\sqrt{L}}{N}\right) \quad , \tag{4.3}$$

where $P(\cdot)$ is the power spectrum of the time series.

The estimator of the bispectrum given by Eq. (4.2) is an element of a complex Wishart with dimension 3 and degrees of freedom L. Asymptotically it has a complex Gaussian distribution.

The bispectrum can be normalized to produce a quantity whose asymptotic statistics can more easily be calculated. Since the asymptotic distribution of the estimator given by Eq. (4.2) is complex Gaussian, the distribution of the normalized bispectrum given by

$$\chi^2(j,k) = \frac{2|\hat{B}(j,k)|^2}{\text{VAR } \hat{B}(j,k)} \tag{4.4}$$

is asymptotically noncentral chi-square with two degrees of freedom and noncentrality parameter

$$\lambda(j,k) = \frac{2L}{N}\gamma(f_j,f_k) \quad , \tag{4.5}$$

where

$$\gamma(f_j,f_k) = \frac{|B(f_j,f_k)|^2}{P(f_j)\,P(f_k)\,P(f_{j+k})} \tag{4.6}$$

is called the skewness function. If the time series is Gaussian, its skewness function will be zero for all frequency pairs and the distribution of the normalized bispectrum is just a central chi-square with two degrees of freedom (the noncentrality parameter will be zero). For perfectly coherent narrowband harmonics, the skewness function is equal to N, the DFT size.

4.2 DETECTION OF HARMONIC COMPONENTS USING THE BISPECTRUM

For the detection of signals in the presence of additive Gaussian noise, the threshold $T(\alpha)$ that would be applied to the normalized bispectrum estimate to detect a nonzero bispectrum at a specified false alarm rate α is determined from the central chi-square distribution. The threshold that would be applied to the magnitude squared of the unnormalized bispectrum estimate is related to the normalized threshold by

$$T_{un}(\alpha) = \frac{NP^N(f_j)P^N(f_k)P^N(f_{j+k})}{2L}T(\alpha) \quad . \tag{4.7}$$

It is shown in Hinich and Wilson (1990) that if a signal with bispectrum $B_s(f_j,f_k)$ and power spectrum $P^S(f)$ is processed in the presence of additive Gaussian noise with power spectrum $P^N(f)$, the normalized bispectrum estimate of signal-plus-noise is noncentral chi-square distributed with a noncentrality parameter given by

$$\lambda(j,k) = \frac{2L}{N\,(1+r^{-1}(f_j))(1+r^{-1}(f_k))(1+r^{-1}(f_{j+k}))}\,\gamma_s(f_j,f_k) \quad , \tag{4.8}$$

where γ_s is the skewness function of the signal and r is the signal-to-noise power ratio:

$$r(f) = \frac{P^S(f)}{P^N(f)} \quad . \tag{4.9}$$

The probability of detection can be computed for the normalized bispectrum from the noncentral chi-square distribution using the noncentrality parameter given by Eq. (4.8) and the threshold $T(\alpha)$. For the magnitude squared of the unnormalized bispectrum, the probability of detection can be calculated from the noncentral chi-square distribution by evaluating the probability that a noncentral chi-square random variable with noncentrality parameter given by Eq. (4.8) will exceed a threshold given by

$$\frac{T(\alpha)}{(1+r(f_j))\,(1+r(f_k))\,(1+r(f_{j+k}))} \quad , \tag{4.10}$$

where $T(\alpha)$ is the threshold for the normalized bispectrum.

From a detection point of view, the issue is how large the normalized bispectrum statistic given by Eq. (4.4) has to be in order to confidently reject the Gaussian noise only hypothesis and assert that a non-Gaussian signal is present. Shown in Fig. 4.1 is a plot of the probability of false alarm as a function of the normalized bispectrum value based on the central chi-square distribution function. The plot is approximately linear on a log false alarm scale with a slope of 4.6 per decade. To operate at a false alarm rate of 10^{-3}, one would reject the hypothesis that only noise is present (the normalized bispectrum statistic is central chi-square distributed rather than noncentral chi-square distributed) for values of the normalized bispectrum statistic that are 13.8 or larger. Since the mean value of the normalized bispectrum statistic is equal to the noncentrality parameter, then the noncentrality parameter must be 13.8 or larger to achieve detection at this false alarm rate.

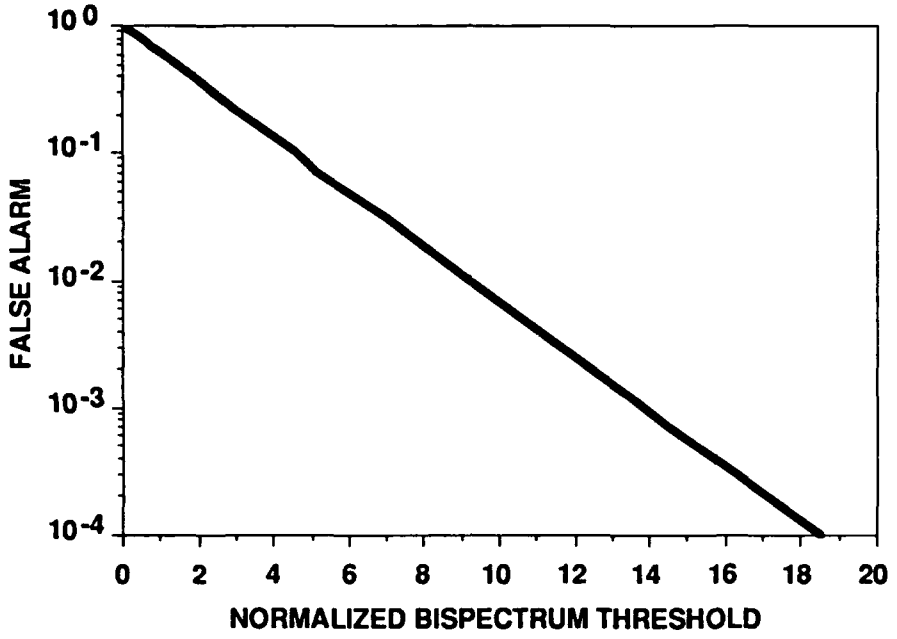

FIGURE 4.1
FALSE ALARM PROBABILITY AS A FUNCTION OF NORMALIZED BISPECTRUM THRESHOLD

From Eq. (4.8) it can be seen that several factors contribute to the value of the noncentrality parameter. One is the skewness function γ_s which is a characteristic of the signal, one is the signal-to-noise ratio r which is a characteristic of the signal and noise power levels, and the rest are characteristics of the processing. Given that a signal has a non-zero skewness function, then there is a tradeoff between signal-to-noise ratio and processing parameters that determines if the nonzero skewness will result in a sufficiently large noncentrality parameter to allow its detection at a given false alarm rate. For small values of the skewness function, the processing parameters and signal-to-noise ratio have to be such that their product, given by Eq. (4.8), remains large enough to produce a sufficiently large noncentrality parameter for detection. The noncentrality parameter has a linear dependence on the number of temporal averages L and an approximately cubic dependence on signal-to-noise ratio (for low signal-to-noise ratios). This implies that if the signal-to-noise ratio decreases by a factor of 2 (3 dB), then it is necessary to increase the number of temporal averages by a factor of 8 in order to retain the same level of detectability.

Equation (4.8) demonstrates the essential relationship between signal characteristics, noise characteristics, and processing parameters that determines the detection performance of the bispectrum. To determine the viability of bispectrum processing for detection of non-Gaussian or nonstationary signals, it is essential to know the skewness function of signals of interest. Given a skewness function, the processing parameters necessary to achieve detection as a function of signal-to-noise ratio can then be determined. For the detection of narrowband harmonics, the skewness function is equal to the DFT size N for perfectly coherent signals. It should also be noted that Eq. (4.8) is relevant for "narrowband" detection, i.e., detection at a single point in the bispectrum. One can also consider "broadband" detection in which the detection statistic is based on bispectrum values over the entire principal domain (Hinich and Wilson, 1990).

Figure 4.2 shows a comparison of the detection performance of both the normalized and unnormalized bispectrum to the power spectrum for detecting harmonics in Gaussian noise. In this plot the three harmonics all have the same signal-to-noise ratio, which is indicated on the horizontal axis of the plot. The number of averages used to generate these results was 10. Because of the limited number of averages, the asymptotic statistics used to produce these results are only approximate. However, these were used because the expression for the exact distribution has not been derived. As can be seen, the unnormalized bispectrum performs better than the power spectrum and the normalized

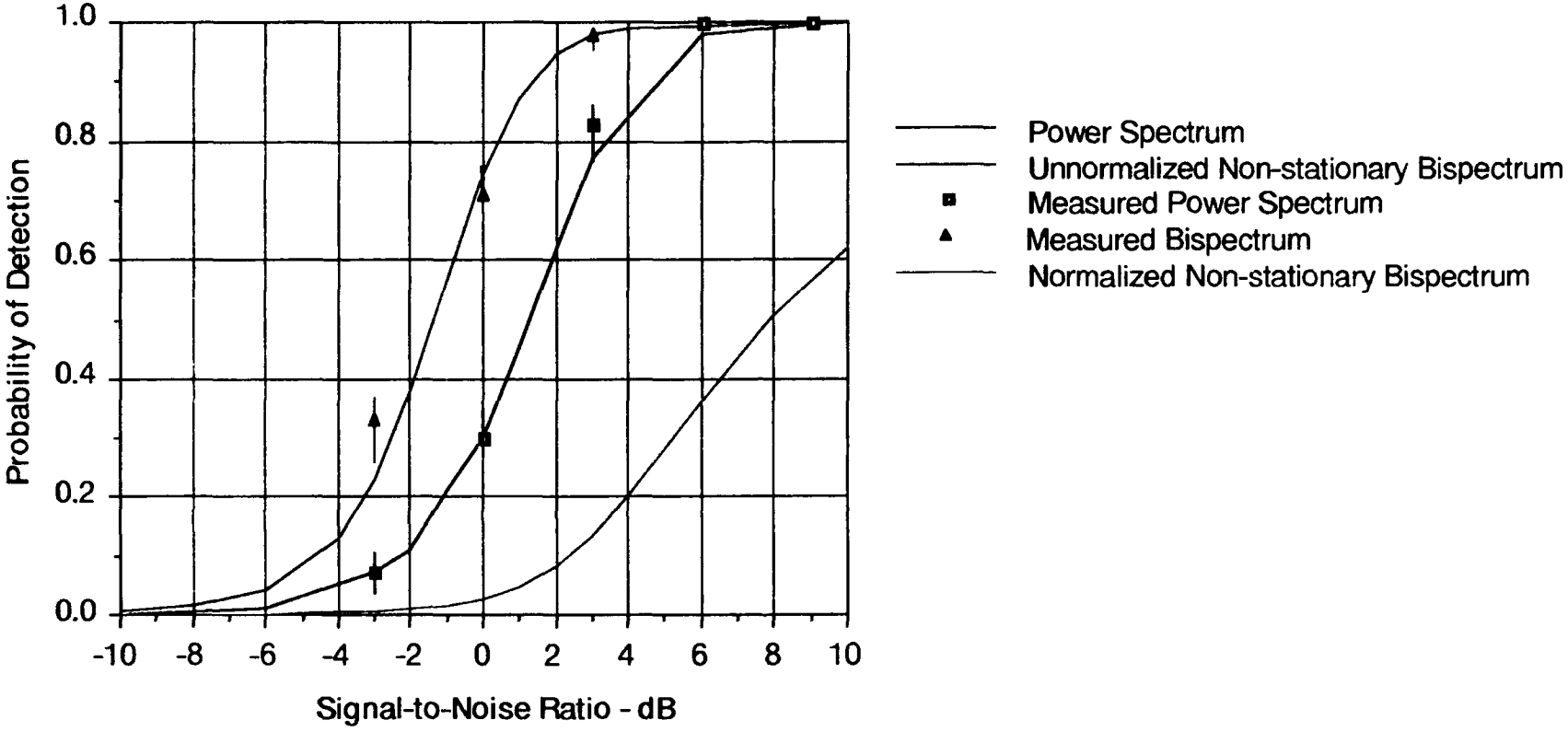

FIGURE 4.2
COMPARISON OF BISPECTRUM AND POWER SPECTRUM
NARROWBAND DETECTION PERFORMANCE

AS-91-134

bispectrum performs worse than the power spectrum. This general result was also seen with the spectral correlation. Also shown are the measured probabilities of detection for the unnormalized non-stationary bispectrum and for the power spectrum using the same data as described for the spectral correlation comparison in Fig. 3.2. As can be seen, the experimentally determined detection probabilities agree well with the predicted detection probabilities, suggesting that the asymptotic non-stationary bispectrum statistics may be adequate for averaging lengths as small as 10.

REFERENCES

Baugh, Kevin W., and Keith R. Hardwicke (1991). "Transient Detection via Spectral Correlation," in preparation.

Brillinger, David R. (1975). Time Series Data Analysis and Theory (Holt, Rinehart, and Winston, Inc., New York).

Hinich, Melvin J. (1982). "Testing for Gaussianity and Linearity of a Stationary Time Series," J. Time Series Analysis 3, 169-176.

Hinich, Melvin J., and Gary R. Wilson (1990). "Detection of Non-Gaussian Signals in Non-Gaussian Noise Using the Bispectra," IEEE Trans. Acoust., Speech, and Signal Proc. 38(7), 1126-1131.

Levanon, Nadav (1988). Radar Principles (John Wiley and Sons, New York).

Nikias, C. L., and R. Pan (1988). "Time Delay Estimation is Unknown Gaussian Spatially Correlated Noise," IEEE Trans. Acoust., Speech, and Signal Proc. 36, 1706-1714.

Papoulis, A. (1965). Probability, Random Variables, and Stochastic Processes (McGraw-Hill Book Company, Inc., New York).

23 April 1991

DISTRIBUTION LIST FOR
ARL-TR-91-8
TECHNICAL REPORT UNDER CONTRACT N00014-89-J-1967

Copy No.

Office of the Chief of Naval Research
Department of the Navy
Arlington, VA 22217-5000
1 Attn: J. Smith (Code 1211)
2 R. Hansen (Code 121)
3 T. Goldsberry (Code 23)
4 N. Gerr (Code 1111)
5 CAPT Fitch (Code 23)
6 G. Remmers (Code 233)

Office of Naval Intelligence
Department of the Navy
Washington, D.C. 20350-2000
7 Attn: L. Long (NIC-00R4)

Commanding Officer
Naval Technical Intelligence Center
4301 Suitland Road
Washington, D.C. 20390
8 Attn: R. Kalny (Code 211)

Commanding Officer
David Taylor Research Center
Bethesda, MD 20084-5000
9 Attn: J. Valentine (Code 1932)
10 B. Douglas (Code 0113)
11 J. O'Donnell (Code 193)
12 N. Keech (Code 1926)

Commanding Officer
David Taylor Research Center Detachment
Puget Sound Naval Shipyard
Bremerton, WA 98314-5212
13 Attn: D. Groutage (Code 1910.2)
14 B. Kipple (Code 1911)

Commander
Space and Naval Warfare Systems Command
Department of the Navy
Washington, D.C. 20363-5100
15 Attn: L. Parish (PMW181T)

Distribution List for ARL-TR-91-8 under Contract N00014-89-J-1967
(cont'd)

Copy No.

	Officer in Charge Naval Underwater Systems Center New London Laboratory New London, CT 06320
16	Attn: R. Tozier (Code 2121)
	Commander Naval Sea Systems Command Department of the Navy Washington, D.C. 20362-5101
17	Attn: R. Dosti (PMS409)
18	Y. Yam (Code 06UR)
	Office of the Asst. Secretary of the Navy (RD&A) Department of the Navy Washington, D.C. 20350-2000
19	Attn: A. Bisson
	Chief of Naval Operations Department of the Navy Washington, D.C. 20350-2000
20	Attn: J. Schuster (OP21T)
	Defense Advanced Research Projects Agency 1400 Wilson Blvd. Arlington, VA 22209-2308
21	Attn: C. Stewart
	Commanding Officer Naval Ocean Systems Center San Diego, CA 92152
22	Attn: C. Persons (Code 732)
	Commander Submarine Development Squadron Twelve Submarine Base New London Groton, CT 06349-5200
23	Attn: NSAP Consultant (Code N2A)
24 - 25	Commanding Officer and Director Defense Technical Information Center Cameron Station, Building 5 5010 Duke Street Alexandria, VA 22314

Distribution List for ARL-TR-91-8 under Contract N00014-89-J-1967
(cont'd)

Copy No.

	Tracor Applied Sciences, Inc. AARD/Sea Operations 35 Thomas Griffin Rd. New London, CT 06320
26	Attn: D. Turbes
	Planning Systems, Inc. 792 S. Westpark Dr. McLean, VA 22102
27	Attn: H. Warner
	Lockheed Missile and Space Corp. O/6580, B/582N 1111 Lockheed Way Sunnyvale, CA 94088-3504
28	Attn: W. Eugene Brown
	Naval Weapons Center China Lake, CA 93555
29	Attn: Gary A. Hewer (Code 39103)
30	Signal Physics Group, ARL:UT
31	Martin L. Barlett, ARL:UT
32	Kevin W. Baugh, ARL:UT
33	Joseph F. England, ARL:UT
34	Douglas J. Fox, ARL:UT
35	Keith R. Hardwicke, ARL:UT
36	Melvin J. Hinich, ARL:UT
37	James L. Lamb, ARL:UT
38	Fredrick W. Machell, ARL:UT
39	Edward J. Powers, ARL:UT
40	Jack H. Sheehan, ARL:UT
41	Ronald O. Stearman, ARL:UT
42	Robert T. Trochta, ARL:UT
43	Gary R. Wilson, ARL:UT

Distribution List for ARL-TR-91-8 under Contract N00014-89-J-1967 (cont'd)

Copy No.	
44	Library, ARL:UT
45 - 70	Reserve, ARL:UT